Multiphase response of palynomorphs to early Toarcian (Early Jurassic) environmental changes in southwest Hungary (Central Europe)

Viktória Baranyi[a*], József Pálfy[b], Ágnes Görög[a], James B. Riding[c], Béla Raucsik[d]

[a]Department of Palaeontology, Eötvös Loránd University, Pázmány Péter sétány 1/C, Budapest H-1117, Hungary

[b]Department of Physical and Applied Geology, Eötvös Loránd University, Pázmány Péter sétány 1/C, Budapest H-1117, Hungary and MTA-MTM-ELTE Research Group for Paleontology, POB 137, Budapest H-1431, Hungary

[c]British Geological Survey, Environmental Science Centre, Keyworth, Nottingham NG12 115GG, United Kingdom

[d]Department of Mineralogy, Geochemistry and Petrology, University of Szeged, Egyetem utca 132, Szeged H-6722, Hungary

*Corresponding author at: Department of Geosciences, University of Oslo, POB 1047 Blindern, 0316 Oslo, Norway

E-mail address: viktoria.baranyi@geo.uio.no (V. Baranyi)

Abstract

Major palaeoenvironmental and palaeoceanographic changes occurred during the late Pliensbachian to early Toarcian (Early Jurassic) leading to the Toarcian Oceanic Anoxic Event (T-OAE) and the perturbation of the global carbon cycle that seriously affected marine ecosystems. The sequence of successive steps of environmental change and regional differences in the unfolding of T-OAE are not yet fully understood, and organic-walled phytoplankton and other palynomorphs are well-suited but underexplored for such studies. Based on the quantitative palynological analyses of thirty-three samples from a black shale-bearing succession in the Réka Valley, Mecsek Mountains, southwest Hungary, five distinctive assemblages are distinguished. These define major shifts in the organic-walled phytoplankton communities and were driven by palaeoenvironmental changes. Palynofacies analysis was also carried out in order to detect changes in the composition of sedimentary organic matter and estimate the terrestrial input.

The lowermost Assemblage 1 is characterized by a moderately diverse phytoplankton community and high levels of terrestrial palynomorphs. In Assemblage 2 a significant peak of the euryhaline dinoflagellate cyst *Nannoceratopsis* is present. This is followed by a dominance of highly opportunistic prasinophytes, coinciding with the temporary disappearance of all dinoflagellate cyst taxa (Assemblage 3). This phytoplankton crisis was followed by a prolonged repopulation phase with low diversity phytoplankton assemblages (Assemblages 4 and 5) and intermittently high levels of terrestrially-derived palynomorphs.

The successive disappearance of individual phytoplankton taxa and the gradual takeover by opportunistic euryhaline species at the onset of the early Toarcian environmental perturbations were related to the establishment of a reduced salinity layer in the surface water, a stable

pycnocline and deterioration of nutrient recycling followed by oxygen deficiency in the water column. The palaeoenvironmental shifts were driven by early Toarcian global warming, which enhanced the hydrological cycle leading to intense runoff and freshwater input into the sedimentary basin of the Mecsek Mountains as evidenced by the high amount of terrestrially-derived palynodebris in the palynofacies.

Comparison with coeval European successions reveals that the palaeoenvironmental changes during the T-OAE were not entirely synchronous, and local factors played a crucial role in influencing phytoplankton communities. Because the Réka Valley section was located in the northwest European epicontinental realm during the Early Jurassic, regional freshening of the surface waters and increased terrestrial input due to the proximity of the hinterland had a greater influence on phytoplankton communities compared to the open oceanic setting of the Tethyan Realm.

Keywords (up to 6)

Toarcian Oceanic Anoxic Event (T-OAE), palynology, palynofacies, dinoflagellate cysts, prasinophytes

Highlights (3-5 lines each up to 85 characters including space)

- Detailed quantitative palynological analysis of a Toarcian black shale succession
- Five intervals record successive changes in organic-walled phytoplankton assemblages
- Peak of the euryhaline genus *Nannoceratopsis*, followed by a dinoflagellate cyst disappearance event
- Changes driven by global warming, enhanced runoff, and freshening of surface waters

1. Introduction

The early Toarcian (Early Jurassic, ~182–178 Ma) was a time of severe palaeoenvironmental perturbations: global warming, sea level rise and the associated geochemical changes in the ocean-atmosphere system created a compound stress of palaeoenvironmental changes which seriously stressed the biosphere and caused biological turnovers. Marine transgression, carbon isotope excursions, other geochemical anomalies and widespread deposition of organic rich sediments are associated with the Toarcian Oceanic Anoxic Event (T-OAE) (e.g. Jenkyns, 1988; McArthur et al., 2000; Schouten et al., 2000; Jenkyns et al., 2002; Bailey et al., 2003; van de Schootbrugge et al., 2005a; Hesselbo et al., 2007; Suan et al., 2008; Littler et al., 2009; Hermoso et al., 2013; Korte & Hesselbo, 2011). A plausible proximal triggering mechanism for the palaeoenvironmental perturbation is methane hydrate dissociation (Hesselbo et al., 2000, 2007), whereas the most likely (and less debated) first-order driver of the paleoenvironmental changes is the emplacement of the Karoo-Ferrar igneous province (e.g. Pálfy & Smith, 2000; McElwain et al., 2005; Svensen et al., 2007; Suan et al., 2008; Burgess et al., 2015). The T-OAE is associated with a second order mass extinction in several taxonomic groups (e.g. Harries & Little, 1999; Pálfy & Smith, 2000; Wignall, 2001; Caruthers et al. 2013; Caswell & Coe, 2013; Danise et al., 2013). Many of these environmental perturbations such as the increased terrestrial input due to enhanced weathering and riverine influx, stratification of the water column and subsequently anoxia in water colum, or acidification of ocean water represent serious stress for many phytoplankton groups. The effects of the oceanic anoxic events on phytoplankton assemblages have been discussed recently (e.g. Bucefalo Palliani et al., 1998, 2002; Bucefalo Palliani & Riding 1999a; Erba, 2004; Mattioli et al., 2004, 2009; van de Schootbrugge et al., 2005b, 2013). Dinoflagellate cysts are one of the major groups of fossilisable phytoplankton groups during Early Jurassic (Stover et al., 1996). They are unicellular algae with two distinct stages in their life cycle.

During the motile stage of the life cycle they inhabit the photic zone and their distribution is affected mostly by surface water temperature, salinity, nutrient availability and light penetration in the photic zone (e.g. Marret & Zonneveld, 2003). Cyst-producing dinoflagellates are very sensitive to the ecological conditions, especially oxygen availability in the bottom waters due to the benthic habitat of their cysts (Anderson et al., 1987). Therefore, due to the planktonic and benthic stages in their life cycle, dinoflagellate cysts provide information on the ecological conditions and physico-chemical properties of both the surface and bottom waters.

Many studies on Early Jurassic dinoflagellate cyst assemblages have focused on their taxonomy, biostratigraphy and palaeobiogeography (e.g. Gocht, 1964; Davies, 1985; Prauss, 1989; Feist-Burkhardt & Wille, 1992; Riding & Thomas, 1992; Bucefalo Palliani & Riding 2003a). The palynological aspects of the T-OAE were first discussed by Bucefalo Palliani et al. (1998; 2002); Bucefalo Palliani & Riding (1999a) and van de Schootbrugge et al. (2005b; 2013). These works aimed at the reconstruction of the palaeoenvironmental changes associated to the T-OAE and were based mainly on dinoflagellate cysts, other organic walled microplankton groups and calcareous nannoplankton. The environmental stress that accompanied the T-OAE caused turnovers among dinoflagellate communities (Bucefalo Palliani & Riding 1999b, Bucefalo Palliani et al., 2002). The genus *Luehndea* and many species either became extinct or temporarily disappeared. The genus *Umbriadinium* probably lost its ability to make fossilisable cysts (Bucefalo Palliani & Riding, 2003b).

The objective of this study is to analyse the changes in organic walled phytoplankton groups (dinoflagellate cysts and prasinophytes) together with changes in the input of terrestrially-derived material, on the basis of palynological investigation and palynofacies analysis of a black shale-bearing sequence in the Mecsek Mountains of southwest Hungary. Our aim is to

reconstruct the pattern of biotic turnover associated with the T-OAE. Comparing microplankton turnover patterns from other localities from the Boreal (Germany, UK) and Tethyan (central Italy) realms, we attempt to elucidate the regional and the global trends in organic walled phytoplankton community change and to assess the overprint on regional palaeogeographical setting on global phenomena. In addition, we record the changes in palynofacies patterns in the T-OAE (Dybkjær, 1991; Tyson 1993, 1995; Feist-Burkhardt et al., 2008; Götz et al., 2008).

2. Geological setting

The Mecsek Mountains are situated in the southwestern part of the Pannonian Basin in Hungary (Fig. 1A). They form the only exposed part of the Mecsek Zone structural unit that belongs to the Tisza Mega-unit (e.g. Csontos & Vörös, 2004; Haas & Péró, 2004) (Fig. 1B). The latter consists of tectonic blocks of the European continental plate that were accreted during the Variscan orogeny and broke off the southern margin of the European Platform (Fig. 2). The Tisza Mega-unit reached its present-day position after a series of drifting and rotation events during the Palaeogene and Neogene (e.g. Csontos et al., 1992; 2002).

During the Triassic and Early Jurassic, the Mecsek Basin was located east of the Bohemian Massif and was an epicontinental depocentre (e.g. Haas & Péró, 2004) (Fig. 2). The Mecsek Basin was situated close to the continental margin and was therefore exposed to significant terrigeneous influence (e.g. Bleahu et al., 1994).

The Upper Triassic to lowermost Jurassic succession is characterised by fluvial, lacustrine, coal-bearing swamp and deltaic deposits of the Mecsek Coal Formation (e.g. Szente, 2012) (Fig. 3). The early Sinemurian eustatic sea level rise coincided with rapid subsidence of the Mecsek Basin and led to a decrease of terrigenous input and deepening of the depositional

environment, reflected by the Vasas Marl Formation (e.g. Császár et al., 2007; Raucsik, 2012a) (Fig. 3). During the late Sinemurian and Pliensbachian, terrigeneous material mixed with biogenic carbonate was deposited in this open marine, deep basin and formed an intensely bioturbated lithofacies, assigned to the Hosszúhetény Calcareous Marl Formation (Fig. 3). This unit is informally known as spotted marl, and it is the equivalent of "Fleckenmergel" or "Allgäu" facies known elsewhere in the European margin of the Neotethys (e.g. Adámek, 2005; Horváth & Galácz, 2006; Raucsik, 2012b). Interbeddded turbiditic sandstone, bituminous limestone and crinoidal limestone occur within the monotonous upper Pliensbachian hemipelagic spotted marl series, suggesting variable control of tectonism, sea level fluctuations and climate change (e.g. Raucsik & Varga, 2008a). The organic-rich silty and clayey marls of the lower Toarcian Rékavölgy Siltstone Formation mark the establishment of suboxic/anoxic conditions in the Mecsek Basin (Raucsik, 2012c) (Fig. 3). The T-OAE is represented by a ~12 m thick black shale succession (Dulai et al., 1992; Raucsik, 2008, 2012c). Overlying the black shales, sedimentation of the "spotted marl" recommenced and continued to the latest Bajocian (the Komló Calcareous Marl Formation) (Raucsik, 2012d) (Fig. 3). Marked changes took place in the sedimentation in the Mecsek Basin during the Middle Jurassic. The amount of terrigeneous input dramatically decreased; and together with the accelerated subsidence, it led to the formation of a deep pelagic basin (Horváth & Galácz, 2006) related to the separation of the Tisza Mega-unit from the European plate due to the opening of the Penninic oceanic branch.

3. Stratigraphy of the Réka Valley section

Jurassic strata are exposed only in the eastern part of the Mecsek syncline (Némedi Varga, 1998) (Fig. 1A, B). The section studied is located near the NE-SW trending Réka Valley, south of Óbánya (Fig. 4). The ~12 m thick black shale succession crops out in a small

tributary ravine. The section was described in detail by Galácz (1991), Dulai et al. (1992) and Raucsik &Varga (2008a, b). The lower part of the section exposes the alternating series of intensely bioturbated calcareous and clayey marl beds ("spotted marl") with intercalations of mixed carbonate-siliciclastic lenses (Fig. 5). The "spotted marl" succession is followed by the black shale beds consisting of light brown to dark grey bituminous shale and greyish clayey marl layers with distinct lamination at some levels (Raucsik, 2008). In the upper part of the black shale interval, intercalations of calcareous-siliciclastic turbidite beds occur. In the black shale beds, pyrite moulds, framboids, fish remains, bivalves and fragmentary plant remains are common (Dulai et al., 1992; Raucsik, 2008). Above the black shale "spotted marl" deposition resumed (Fig. 5).

Ammonites (*Hildaites* cf. *siemensi*, *H.* cf. *levisoni*, *H.* cf. *gyralis*) from the black shales, as well as *Harpoceras* cf. *exaratum* found directly above the topmost black shale layers, indicate the lower Toarcian *Harpoceras falciferum* ammonite biozone (Galácz, 1991). However, due to the sporadic occurrence of index species, especially ammonites, the base of the Toarcian is not well defined and the exact position of the boundary between the *H. falciferum* and *Dactilyoceras tenuicostatum* ammonite biozone remains controversial (Galácz, 1991; Dulai et al., 1992; Baldanza et al., 1995; Varga et al., 2009). Based on calcareous nannoplankton, Baldanza et al. (1995) placed the boundary between the *H. falciferum* and *D. tenuicostatum* ammonite biozones several metres above the base of the black shales (Fig. 5) In sample BS 15 (1 m below sample BS 16), Mattioli (pers. comm.) found the calcareous nannoplankton *Carinolithus poulnabronei*, which often occurs together with *C. superbus* in early Toarcian assemblages and correlates with the *D. tenuicostatum* ammonite biozone. Sample BS 59 (1 m above sample BS 58) yielded *Watznaueria fossacincta* and *W. colacicchii*. The first appearance of these species is usually coincident with the first occurrence of *Discorhabdus*

striatus, suggesting correlation with the topmost part of the *H. falciferum* ammonite biozone (Mattioli & Erba, 1999).

Previously, dinoflagellate cyst assemblages of the Réka Valley section were investigated by Baldanza et al. (1995) and Bucefalo Palliani et al. (1997). Their work focused mainly on the taxonomy, biostratigraphy and palaeogeographical implications of the dinoflagellate cysts. The species *Luehndea cirilliae* and *Luehndea microreticulat*a were first described from the Réka Valley section (Bucefalo Palliani et al., 1997). The total organic carbon (TOC) values of the sediments vary from 3.89 to 8.12% in the oil shales, and 2.14-3.29% in the clayey marl beds (Varga et al., 2007). Investigation of samples from the lower 5 m of the black shale succession show that the organic particles are almost exclusively composed of liptinite formed mainly from marine material, especially algae (Varga et al., 2007). The carbon isotopic composition of the kerogen fraction ranges from -30.9‰ to -28.6‰ relative to V-PDB (Varga et al., 2007). These values are slightly less negative than in other Toarcian organic-rich formations (e.g. Schistes Carton, Posidonia Shale, Jet Rock) during the carbon isotope excursion of the T-OAE, but sampling here was of low resolution and pre- and post-excursion background levels from the underlying and overlying strata are subject of ongoing high-resolution studies. The carbon and oxygen isotopic composition of the carbonate fraction has been altered by diagenesis; therefore they cannot be used in palaeoenvironmental interpretations (Varga et al., 2007). The clay mineralogical composition of the black shales is dominated by kaolinite (Raucsik & Varga, 2008a, b), which is typical of strongly leached soils that become progressively enriched in aluminium (van de Schootbrugge et al., 2009) indicating extreme continental weathering rates in the source area related to a humid, tropical-subtropical climate conditions (Branski, 2010).

4. Material and methods

Thirty-three samples from the Réka Valley outcrop were analysed herein (Fig. 5). Palynomorphs from the black shale sequence were extracted from the same samples (labelled BS 2-58) collected by Varga et al. (2007) and Raucsik & Varga (2008a, b). Additional palynology samples were collected from strata below and above the black shale (labelled RV 1-20). All the samples were prepared using standard palynological processing techniques, including 36% HCl and concentrated HF for the dissolution of carbonate and silicate minerals respectively (Wood et al., 1996). For density separation, $ZnCl_2$ (density 2.2 g/cm^3) was used. In order to reduce the amount of amorphous organic matter (AOM), the black shale samples were oxidised using either NaOH, a mixture of NaOH and HNO_3, or Schulze's solution (a mixture of the aqueous solution of $KClO_3$ and concentrated HNO_3). The microscope slides were mounted in glycerine jelly. The relative percentage of palynomorphs is based on counting approximately 200 grains in 2 to 4 microscope slides. Sample RV 5 proved barren, and samples BS 48, BS 46, BS 44, RV 17, RV 19 and RV 20 were sparse, i.e. less than 30 specimens were recovered. Dinoflagellate cysts were reasonably diverse and moderately well preserved. By contrast, terrestrial palynomorphs were highly diverse and generally well-preserved with a colour index of 1–2 on the thermal alteration scale of Batten (2002). The relative abundance of palynomorphs was calculated and plotted using the Tilia/TiliaGraph computer program (Grimm, 1991–2001). Palynomorph assemblages were defined with constrained cluster analysis using CONISS (Grimm, 1987) within Tilia (Fig. 6). Palynofacies analysis was performed in order to determine the type and preservational state of the sedimentary organic matter, plus the amount of terrigenous input. The subdivision of the palynofacies groups and their terminology was done using the method of Oboh-Ikuenobe & de Villiers (2003) (Table 1). Four palynofacies parameters were calculated on the basis of counting ~400 organic particles per slide: the ratio of terrestrial to marine palynomorphs (t/m), the ratio of spores to bisccate pollen grains (sp/bs), the ratio of opaque to translucent

phytoclasts (op/tr) and the ratio of bladder or lath-shaped to equidimensional opaque phytoclasts (bl/eq) after Tyson (1993), Pittet & Gorin (1997), Feist-Burkhardt et al. (2008), and Götz et al. (2008) (Table 1) (Fig. 7).

Despite multiple cycles of oxidation treatment, the black shale samples yielded large amounts of AOM that made the identification of palynomorphs and phytoclasts difficult or impossible. AOM was analysed under fluorescent light to evaluate the preservation state of sedimentary organic matter and to distinguish the palynomorphs and phytoclasts that are masked by the AOM in light microscopy. However, fluorescent microscopy was not a suitable method for analysing palynomorphs from the black shale samples, because of the intense autofluorescence of the mounting medium. Furthermore, the intense fluorescent light melts the mounting material and damages the slides. For these reasons, meaningful palynofacies analyses could only be carried out on the underlying and overlying units; results from the black shale succession would not be reliable and comparable to the other samples. Optical microscopy was performed in the Department of Palaeontology, Eötvös Loránd University, Budapest, Hungary using a Nikon Eclipse E600 microscope. The fluorescence microscopy was undertaken at the Department of Botany, Hungarian Natural History Museum with a Nikon Eclipse E600 equipped with a fluorescent light source. All samples, residues and microscope slides, including the figured specimens (Plates I–III), are curated at the Department of Palaeontology, Eötvös Loránd University.

Data analysis and the calculation of the diversity indices were carried out using the PAST software package 3.01 (Hammer et al, 2001). Samples containing <30 specimens were excluded from the data analyses. For each sample, the diversity of the marine phytoplankton was measured using the Simpson Diversity Index (1-D). This is a suitable method for assessing diversity changes throughout the section, because the abundance of palynomorphs is heterogenous. The Simpson Diversity Index takes into account the number of taxa present. It

ranges between zero for monospecific assemblages and 1 where all taxa are equally dominant. The index assesses the probability that two individuals randomly selected from a sample will belong to a different taxon and the greater the 1-D value, the greater the diversity (Danise et al. 2013). The Simpson Diversity Index was calculated only for marine taxa, because the reconstruction of changes in terrestrial vegetation pattern was beyond the scope of this study. Detrended correspondence analysis (DCA) performed with PAST (Hammer et al., 2001) was used in order to determine similarities between the samples studied (Hill & Gauch, 1980). The aim was to detect relationships between the different palynomorph groups, with special emphasis on co-occurrences of different algal groups in the organic-walled microplankton community and to characterize palaeoecological changes (Correa-Meitro et al., 2014). A taxon abundance matrix was used for the input of data. The advantage of DCA compared to other ordination methods is the elimination of the arch effect (Hill & Gauch, 1980; Hammer et al., 2001), and that the analysis is less affected by smaller differences in sample size (i.e palynomorph counts) or diversity (De Toledo et al., 2009).

5. Results

5.1 Palynomorph assemblages, Simpson Diversity Index and palynofacies

Dinoflagellate cysts dominate the marine palynomorphs (Plate I). Acritarchs occur throughout the succession, although in low abundance and diversity; they are represented by only three genera. Four taxa are of prasinophytes were distinguished. These include small (10–15 µm diameter), thin walled, spherical palynomorphs, commonly referred to as sphaeromorphs, and which are characteristic of the black shale samples (Palte III). The terrigenous fraction contains trilete spores, bisaccate pollen, non-saccate gymnosperm pollen grains and *Classopollis* sp. The spores (Plate II) belong to ferns, lycopods and mosses; the 21 taxa identified belong to 19 genera, and 15 taxa were determined at the species level. Smooth

trilete spores assigned to the ferns (*Cyathidites* spp.) are predominant. Ornamented forms are less frequent, although *Ischyosporites variegatus* and *Manumia delcourtii* are common in some samples. Gymnosperms (Plate II) are represented by four taxa of bisaccate pollen grains (*Alisporites robostus*, *Alisporites* cf. *thomasii*, *Pytiosporites* sp. and *Vitreisporites pallidus*). Non-saccate pollen grains (*Cerebropollenites* sp., *Chasmatosporites* spp., *Monosulcites* spp. and *Spheripollenites psilatus*) were recorded sporadically. The general aspect of the sporomorphs is characteristic of the late Pliensbachian to early Toarcian of Europe (van Erve, 1977; Lund & Pedersen, 1984; Guy-Ohlson, 1986; Dybkjær, 1991; Bucefalo Palliani, 1997). On the basis of changes in the diversity and composition of palynomorphs in the section studied, the following five successive assemblages were distinguished in the cluster analysis (Fig. 6), each of them is also characterised by their distinctive palynofacies.

5.1.1 Assemblage 1

In samples RV 1 to RV 7, marine palynomorphs are present in higher proportions than spores and pollen grains, the t/m index is <1 except in RV 6, where its value reaches 1.69 (Figs 6, 7). Species of the genus *Luehndea* are predominant among the dinoflagellate cysts. *Luehndea spinosa* (Plate I, Fig. 12) and *L. cirilliae* are frequent, whereas *L. microreticulata* (Plate I, Figs 9-10) is rare. Other dinoflagellate cyst taxa, e.g. *Mancodinium semitabulatum*, *Mendicodinium* spp., *Umbriadinium mediterranense* and *Valvaeodinium* spp. and indeterminate dinoflagellate cysts are rerelatively rare. Prasinophyte phycomas and the sphaeromorphs are only minor constituents of the palynomorph assemblage (3–6%). The Simpson Diversity Index is around 0.8 in Assemblage 1 indicating that the phytoplankton communites have a relatively even species distribution (Fig. 6). Within the terrestrial fraction, gymnosperm pollen grains are dominant. The palynomacerals comprise sedimentary organic

matter of mixed terrestrial and marine origin (Plate III, Fig. 5), opaque phytoclasts form the dominant fraction (82.5% on average), palynomorphs are subordinate (Fig. 7).

5.1.2 Assemblage 2

Samples RV 8 and RV 9 are distinguished by a greatly increased proportion of *Nannoceratopsis* (Fig. 6). This genus represents 99% of the dinoflagellate cyst association and 66% of the total palynomorph spectrum. The diversity falls to 0.3 suggesting community changes among organic walled phytoplankton (Fig. 6). *Nannoceratopsis gracilis* includes many different morphotypes including many with well-defined dorsal antapical horns and strongly reduced ventral antapical horns. Morphotypes 13 and 17 of Gocht (1964) are common. These forms (Plate I, figs 4-5) are similiar to *N. gracilis* subsp. *obsoleta*, which is characteristic in the early Toarcian of Germany. Some specimens are close to *N. magnicornus* (Plate I, fig. 11). A few forms with characteristic rectangular outlines, prominent dorsal antapical horns and reduced ventral antapical horns occur (Plate I, fig. 6). Specimens with antapical horns of equal length are less frequent. *Luehndea spinosa* is recorded in RV 9, this is the highest occurrence of the species in the section investigated. The stratigraphical range of this species is late Pliensbachian to earliest Toarcian, from the *Pleuroceras spinatum* to the *D. tenuicostatum* ammonite biozone (Bucefalo Palliani et al., 1997). The ratio of the sphaeromorphs increased. The t/m index is low, 0.06 and 0.25 respectively, but in the terrestrial fraction the ratio of spores to bisaccate pollen is higher compared to assemblage 1 (2.75 and 1.00 respectively) (Fig. 7). The relative proportion of trilete spores and *Classopollis* sp. to the bisaccate pollen grains is higher than in Assemblage 1. In the palynofacies (Plate III, fig. 6) opaque phyoclasts are dominant, but there is no consistency in the shape and size

distribution of opaque phytoclasts. Equidimensional and lath-shaped particles are both present (Fig. 7). Amorphous organic matter is absent in these samples.

5.1.3 Assemblage 3

In the samples from the black shale, the abundance of all palynomorph groups abruptly drops, with the exception of the sphaeromorphs that are the major constituents of this assemblage (Fig. 6). The severe crisis is reflected in the extremely low 1-D values ranging between 0.04 and 0.33. Sample BS 32 with relatively high 1-D values is marked by a moderately high diversity of prasinophytes, where different species of *Tasmanites* and sphaeromorphs are present. The sphaeromorphs occur as single grains, in clusters, or in chains (Plate III, figs 1-2). Dinoflagellate cysts are virtually absent in this assemblage. Prasinophytes are represented by several taxa (*Cymathiosphaera pachytheca*, *Leiosphaeridia* sp., *Pleurozonaria polyporosa* and *Tasmanites* sp.). In sample, BS 2 a few dinoflagellate cysts also occur, although the poor preservation of these specimens prohibited their accurate determination. The percentage of each palynomorph group is 1–3%, except for the sphaeromorphs, which make up 93% of the total palynomorph assemblage. Sedimentary organic matter is represented mostly by AOM (Plate III, figs 3-4). This amorphous material is homogenous in light microscopy, although fluorescent light reveals that the amorphous clusters mask prasinophytes, phytoclasts sphaeromophs and sporomorphs (Plate III, fig. 3). The fluorescence of the AOM is very weak, from pale brown to yellowish green, in contrast to the palynomorphs and phytoclasts that are brightly fluorescent. The fluorescence colours of both palynomorphs and phytoclasts are yellow to green (Plate III, figs 3-4).

5.1.4 Assemblage 4

The terrestrial fraction of Assemblage 4 abruptly increased in the beds overlying the black shale. In samples RV 11 to RV 15, the ratio of trilete spores (e.g. *Cibotiumspora jurienensis, Concavisporites mesozoicus, Cyathidites* spp., *Dictyophyllidites harrisii* and *Ischyosporites variegatus*) significantly increased, associated with a high levels of terrestrial phytoclasts (Figs 6, 7). The spores/bisaccate pollen ratio is between 5.0 and 5.5. The reappearing microplankton assemblages are very poor, dinoflagellate cysts and acritarchs are rare. Their scarcity may be due to the diluting effect of sporomorphs and phytoclasts. Dinoflagellate cysts are represented only by a few specimens of *Nannoceratopsis senex* (Plate I, fig. 1). Prasinophycean algae are common, and the sphaeromorphs still occur in significant numbers (average 83%), but they show a decreasing trend in samples from RV 10 to RV 12 and they never form clusters or chains. The t/m index still remains low, as the sphaeromorphs are still common. Small aggregates of AOM are present in samples RV 13 to RV 15, but in the rest of the samples, no AOM was recorded. In the palynofacies, the translucent phytoclasts are dominant, which exhibit great variety in colour, shape and size (Fig. 7).

5.1.5 Assemblage 5

The dominance of the terrestrial fraction characterises the palynomorph assemblages in samples RV 16 to RV 20; the marine fraction is still impoverished (Fig. 6). Dinoflagellate cysts consitute around 4% of the marine palynomorphs in each sample. The first occurrence of *Nannoceratopsis spiculata* (Plate I, fig. 13) is recorded in sample RV 20, which already indicates the *Hildoceras bifrons* ammonite biozone (Riding & Thomas, 1992). The proportion of acritarchs (6%) is higher than in Assemblage 4. The Simpson Diversity Index of the phytoplankton assemblages do not reach the values that were characteristic before the event

(Fig. 6). Prasinophyte phycomas occur in significant numbers (21%), but the sphaeromorphs are absent. The sporomorphs are the dominant fraction of the palynomorph assemblages, with spores being most abundant. The sporomorphs from Assemblages 4 and 5 do not show marked compositional changes in comparison. Although the ratio of bisaccate pollen to trilete spores is higher in comparison to Assemblage 4 (Figs 6, 7). Despite the similar composition of palynomorph assemblages, the differences in the palynofacies allow the differentiation of the two assemblages. An increase of opaque, equidimensional phytoclasts is documented in this part of the section and the total absence of AOM (Plate III, Fig. 8) (Fig. 7). The marine fraction is somewhat higher than in Assemblage 4, but the t/m index is also still high with an average of 4.31 due to the impoverished phytoplankton communities.

5.2 *Multivariate data analysis*

To further test the palaeoecological signal of the palynomorph groups investigated, a multivariate method, detrended correspondence analysis (DCA) was applied to the taxon abundance distribution matrix (Fig. 8). In the DCA scatter plot, four major groups of samples are distinguished (Fig. 8). This grouping compares well with the previously established palynomorph assemblages, except that Assemblage 3 and 4 could not be separated using DCA due to the predominance of the sphaeromorphs in both assemblages. Assemblages 3-4 and 1 display a strong polarisation along Axis 1 (Fig. 8): Assemblages 3-4 were placed on the left side, whereas Assemblage 1 on the far right side of the field (Fig. 8). Similarity of Assemblages 1 and 5 is manifested in their close placement in the DCA plot, but they are clearly separated from the samples of Assemblage 2 (RV 8, RV 9), which plot to the upper right field with high values along Axis 2, owing to high proportions of *Nannoceratopsis* compared to the rest of the sample population. In DCA analyses, the elimination of the arch effect by the division of the ordination into segments distorts the variance fractions and the

eigenvalues of the different axes cannot be interpreted as variance fractions (Hill & Gauch, 1980; Legendre & Legendre, 1998). The eigenvalues, by contrast, reflect the relative importance of the different axes (Legendre & Legendre, 1998; Correa-Metrio et al., 2014), in this case the eigenvalue of Axis 1 is 0.7088, that of Axis 2 is 0.3481. Changes along Axis 1 account for the majority of the variance within the data. Sphaeromorphs and prasinophytes are characterized by low scores, in contrast to dinoflagellate cysts and terrestrial palynomorphs which show high values along Axis 1 (Fig. 8). On Axis 2, sphaeromorphs and *Nannoceratopsis* have very high positive values, whereas all other dinoflagellate cyst taxa, the terrestrial palynomorphs (except spores) and the acritarchs scored negative values. Comparing row scores, samples from Assemblage 1 have very high values on Axis 1 and low values on Axis 2. Axis 1 values decrease towards Assemblage 2 and reach their minimum in the samples from Assemblage 3 (Fig. 8).

6. Discussion

The phytoplankton communities responded to the palaeoenvironmental stress associated with the T-OAE with successive replacement of characteristic assemblages. The succession is divided into five palynomorph assemblages (Fig. 6) that represent different intervals in the progression of palaeoenvironmental perturbation, driven by changes in oxygen level, salinity and nutrient supply in the water column. These intervals reflect changes in the paleocommunities that can be interpreted using the framework of four successive stages recognized in modern ecosystems affected by anoxia: (1) undisturbed, climax communities, (2) transitional communities, (3) disturbed communities and (4) severely disturbed communities (Danise et al., 2013). Three of these communities (2 to 4, see above) are unequivocally present in the Réka Valley succession.

6.1 Phytoplankton community changes

Interval 1 (samples RV 1–RV 7)

Strong terrestrial influence and presumably eutrophic conditions are inferred from the palynofacies and the palynomorph distribution in Interval 1. The most abundant dinoflagellate cysts *Luehndea spinosa* and *Nannoceratopsis gracilis* are deemed to be opportunistic species, which may have favoured higher nutrient levels from high terrigenous input (Bucefalo Palliani & Riding 1997a, b; 2000). This assemblage has the highest Simpson Diversity Index values (0.7–0.85) within the succession (Fig. 6). Assemblage 1 represents a transition from an undisturbed, climax community to a disturbed association (Assemblage 2), which is manifested in the increased number of opportunistic species and higher bioproductivity. It is assumed that a true undisturbed climax community was not recorded in the succession studied, as all assemblages were characterised by moderate to low diversities, but high abundance values.

Warm, humid palaeoclimate and significant riverine influx are inferred from the presence of spores (e.g. *Cibotiumspora juriensis, Cyathidites* spp., *Dictyophyllidites harrisii, Ischyosporites. variegatus, Manumia delcourtii, Neoraistrickia* sp. and *Uvaesporites argentaeformis*) in the terrestrial fraction of the palynomorphs. The strong heterogeneity of phytoclasts in terms of particle type (i.e. brown wood, charcoal, cortex, cuticle fragments and membranous tissues), shape and size (Fig. 7) is also explained by intense riverine input resulting from enhanced runoff from the hinterland (Dybkjær, 1991). This scenario is consistent with the general global warming and humid climate, intensification of continental weathering and enhanced runoff from the hinterland during the early Toarcian (e.g. McElwain et al., 2005; Dera et al., 2009). Increased weathering is also supported by the high kaolinite content in the clay mineral spectrum of the section (Raucsik & Varga, 2008a, b). The absence

of AOM in these samples indicates ventilated, well-oxygenated bottom conditions and an unstable water column with vertical mixing of nutrients.

Interval 2 (samples RV 8–RV 9)

The abundance of *Nannoceratopsis* spp. in Interval 2 marks a significant disturbance of the phytoplankton communities. *Nannoceratopsis* is considered to have been an opportunistic, euryhaline dinoflagellate cyst genus (e.g. Riding, 1983; 1984; 1985; 1987) that could readily adapt to lower salinity conditions in the surface waters caused by the increased freshwater input. The low Simpson Diversity Index values (0.3–0.5) (Fig. 6) also suggest that this assemblage represents a disturbed community. Several abberant morphotypes of *Nannoceratopsis gracilis* occur in Interval 2. Some of these are similar to *N. magnicornus* (recorded from the *Dactylioceras tenuicostatum* ammonite biozone in France; Bucefalo Palliani & Riding, 1997a), some resemble *N. gracilis* subsp. *obsoleta* (*Pleuroceras spinatum* to *Hildoceras bifrons* ammonite biozones in Germany; Prauss, 1989), yet others exhibit a rectangular outline and one prominent dorsal antapical horn (Plate I, fig. 6.). These morphotypes are confined to Interval 2; in Interval 1 or higher in the section *Nannoceratopsis* is represented by other taxa. The appearance of these unusual forms is indicative of stressed palaeoenvironments and represents the reaction of this genus to lower surface water salinity and/or changes in oxygen and nutrient availability. According to Bucefalo Palliani & Riding (2000), these unusual morphological features of *Nannoceratopsis* reflect the differing tolerance levels of the species. *Nannoceratopsis magnicornus* did not survive the anoxic phase in England, France and Hungary, whereas *N. gracilis* and *N. senex* are still present in higher stratigraphical levels at these localities. It is difficult to determine the advantages or disadvantages of the morphological features of *N. gracilis, N. magnicornus* or *N. senex*. It was probably related to the relationship of size, shape and weight of the cysts to the buoyancy and

hydrodynamic forces in stratified water bodies. Evitt (1961) pointed out the huge intraspecific morphological variability of *N. gracilis* and we suggest that the abberant specimens or variants are all morphotypes of *N. gracilis*. Additionally, studies on many modern dinoflagellates have shown that salinity exerts a strong control on the morphology of their cysts (e.g. Ellegaard, 2000; Mertens et al., 2009; Rochon et al., 2009; Verleye et al., 2012). Intringuingly, Evitt (1961) and Gocht (1972) pointed out the similarities of the epicystal tabulation pattern between peridinoid dinflagellates and *Nannoceratopis*. Although *Nannoceratopsis* belongs to a separate order of dinoflagellates (Fensome et al., 1993) without any modern descendant, it cannot be entirely excluded that they had similar lifestyles to modern peridinoid heterotrophic dinoflagellates (Evitt, 1961), thereby explaining their high productivity and prevalence in eutrophic water masses.

Interval 3 (samples BS 2–BS 58)

The increased freshwater supply during Intervals 1 and 2 led to the establishment of a stable and stratified water column with dysoxic, or anoxic conditions at the sea bed and in the water column. In the palynofacies, the abundance of AOM clearly indicates oxygen deficiency at the sediment-water interface and the lack of bioturbation leading to the deposition of finely laminated, organic-rich black shales. The kerogen of the black shales consists mainly of marine organic material of algal origin (liptinite) with less than 10% terrestrial component (vitrinite and intertinite) (Varga et al., 2007). However, fluorescence analysis has revealed that the AOM masks many sporomorphs and phytoclasts. The temporary presence of euxinic conditions during the deposition of the black shale in the Réka Valley is manifested by the presence of micrometre-scale pyrite framboids in the black shale. The episodic return of oxygenated conditions is suggested by sparse bivalves at some levels of the black shale

(Galácz, 1991). However, based on the estimates of Röhl & Schmid-Röhl (2005) from the Posidonia Shale, these episodes could have lasted only few months or years.

The onset of black shale sedimentation is coeval with a sharp reduction in phytoplankton diversity. The low salinity, oxygen deficiency and subsequently oligotrophic conditions were only tolerated by some phytoplankton groups. The severe disturbance of the phytoplankton communities is also manifested in the low Simpson Diversity Index, which decreased from 0.3–0.5 to 0.05–0.2 (Fig. 6). The marine palynomorph spectrum mainly comprises sphaeromorphs. Previously, these have been proposed to belong to several groups (e.g. pollen grains, green algae, bacteria), but their affinity still remains uncertain (Bucefalo Palliani et al. 2002; van de Schootbrugge et al. 2005b, 2013). According to Prauss & Riegel (1989), their affinity probably lies in the Prasinophyceae, a primitive group of Chlorophyta, which is corroborated by their common occurrence together with prasinopyte phycomas (van de Schootbrugge et al., 2013). The sphaeromorphs, together with other prasinophytes, represent the only phytoplankton groups that could survive the significant freshening of surface waters, or could withstand periods when dysoxic-anoxic, probably even euxinic conditions reached the photic zone. Furthermore, they were better adapted to the reduced recycling of nutrients that sank to the bottom, and could not return to the photic zone again due to density stratification in the water column (Farrimond et al., 1989; Prauss, 2007).

The extension of the oxygen minimum zone severely affected the dinoflagellate cyst assemblages. Studies on modern dinoflagellates have proved that oxygen availability exerts a strong control on the excystment of dinoflagellates, and anoxic conditions completely prohibit the successful germination of the cysts (Anderson et al., 1987; Pross, 2001). This led to the temporary disappearance of dinoflagellates (the “blackout” event *sensu* Loh et al., 1986).

This characteristic association of high relative abundances of sphaeromorphs, AOM and the lack of dinoflagellate cysts is widely recognised the from the lower Toarcian black shale facies in northwest Europe (e.g. Wall, 1965; Wille, 1982; Lund & Pedersen, 1984; Prauss & Riegel 1989; Dybkjær, 1991; Prauss et al., 1991; Bucefalo Palliani et al., 2002). The dinoflagellate cyst diasappearace extends from the upper part of the *D. tenuicostatum* to the *H. falciferum* ammonite biozone. The prasinophytes are considered as disaster taxa because of their peaks in the near absence of other phytoplankton groups like dinoflagellate cysts (van de Schootbrugge et al., 2005b). However, the reasons for their general proliferation during anoxic events, and their widespread distribution at the T-OAE, are still controversial. Prauss (2007) summarised the probable causes of prasinophyte abundance during anoxic events (e.g. the T-OAE and the Cenomanian/Turonian event). He suggested that low salinity of surface waters and the extension of the oxygen minimum zone alone cannot account for the recorded turnover in the phytoplankton communities and the availability of distinct trace elements such as Cu, Fe, Mn, Mo or Zn and nutrients (N, P) may exert a bigger control on different algal groups (Falkowski et al, 2004; Katz et al. 2004). The prasinophyte abundance may also be connected to the denitrfication of the water column (Jenkyns et al., 2001).

Intervals 4 and 5 (samples RV 10–RV 20)

The return of bioturbated sediments (bioturbated marls, calcareous and clayey marls with increasing carbonate content upsection) in the upper part of the section marks the end of the anoxic event, and the re-establishment of an oxygenated water column. However the phytoplankton communities did not yet fully recovered, and represent a disturbed, transitional community to climax assemblages. The Simpson Diversity Index of the phytoplankton continued to remain low (Fig. 6). The Lazarus effect (Wignall & Benton,1999) is a common feature among the dinoflagellate cysts returning in this interval, there are many species which

reappeared after the event. The adaptation of *Nannoceratopsis* to a more proximal setting with lower salinity may have favoured their survival during the T-OAE. They probably used proximal settings as refugia; Prauss (1996) suggested they could thrive in nearshore settings due to their euryhaline nature (e.g. Riding, 1983, 1984, 1987).

This interval is also characterised by an increase of fern spores, whereas other terrestrial palynomorphs occur only in low proportions indicating humid and warm palaeoclimatic conditions. A few dinoflagellate cysts (e.g. *N. senex*) and acritarchs occur, and sphaeromorphs are still present. The absence of AOM indicates a ventilated, non-stratified water column. The palynofacies is dominated by bladed, elongated phytoclasts, plant tissues and cuticles indicating either the proximity of the shoreline, intense runoff or both. In Interval 5, sphaeromorphs further declined and the palynofacies patterns indicate an unstable water column with ventilated conditions. The abundance of predominantly rectangular, small opaque phytoclasts indicates a deepening trend in the late Toarcian of the Mecsek Zone which is consistent with the geological evolution of this area (Csontos & Vörös, 2004).

6.2 Interpretation of the results of the Detrended Correspondence Analysis (DCA)

A scatter plot clearly shows the polarisation of samples along both Axis 1 and Axis 2 placing samples with sphaeromorphs on the far left and samples dominated by other phytoplankton to the right side (Fig. 8). This pattern was caused by the palaeoenvironmental change associated with the T-OAE. Samples with high proportion of *Luehndea* are closer to samples with acritarchs, other dinoflagellate cystss, bisaccate pollen and *Classopollis*, indicating probably generally favourable conditions for the phytoplankton with minor to moderate terrestrial input that supports a diverse community. This is also suggested by the strong difference in the axes scores compared to that of the sphaeromorphs, indicating that the latter group represents

serious palaeoenvironmental deterioration. The *Nannoceratopsis* peak in samples RV 8 and RV 9 records a distinct event of very high nutrient input, likely both from marine and terrestrial source. *Nannoceratopsis* attained relatively high values on both axes of the DCA indicating that its abundance is not only controlled by nutrient availability, but another factor, probably sea surface salinity also exerted significant influence on the group. The position of the different groups and the axes scores suggest that Axis 1 largel
y represents nutrient availability in the water column moving from eutrophic conditions (indicated by the terrestrial input and recycling of nutrients) to oligotrophic conditions due to the establishment of stratified water column. By contrast, Axis 2 probably represents the surface water salinity gradient. Sphaeromorphs are indicative of oligotrophic conditions with restricted nutrient recycling due to a stratified water column, with significant freshening of the water column. The position of the sphaeromorphs in the DCA diagram corroborates the hypothesis of Prauss (2007) that low salinity suface waters and oxygen deficiency in the water column alone cannot account for the abundance of the sphaeromorphs during the T-OAE and that the availability or lack of distinct nutrients exerted a strong control on phytoplankton turnover patterns. The position of *Nannoceratopsis* and its high score on both axes indicates that the peak is associated with the freshening of surface waters and an increase in nutrient levels from a terrestrial source leading to eutrophic conditions. Prasinophytes probably mark the first stage of the deterioration in nutrient recycling and freshening inferred from intense riverine input that could also account for the virtual abundance of spores. *Luehndea* and other dinoflagellate cysts (except *Nannoceratopsis*), acritarchs and gymnosperms (*Classopollis*, bisaccate pollen grains) are grouped together. This is because they represent normal (or close to normal) salinity conditions and explain, with the non-stratified water column and sufficient nutrient input, the contradictory scores on both DCA axes compared to the sphaeromorphs.

6.3 Correlation of phytoplankton turnover events and comparison with other lower Toarcian black shale localities

To elucidate regional and global trends in biotic turnovers among organic–walled phytoplankton communities, four localities have been chosen for comparison with the five stage successive floral replacement pattern observed in the Réka Valley section (Table 2). The Brown Moor borehole in Yorkshire, UK (Bucefalo Palliani et al. 2002); the Bisingen/Zimmern borehole in southwest Germany (Prauss et al., 1991) and the Grimmen section in northwest Germany (Prauss, 1996) were chosen from the the northwest European Realm. From the Mediterranean Tethyan Realm, successions from the Umbria-Marche Basin were selected (Bucefalo Palliani et al., 1998; Bucefalo Palliani & Riding, 1999a). Additinally, the Quercy section in southwest France was also chosen for comparison due to its transitional position between the northwest European epicontinental areas and the Mediterranean Realm (Bucefalo Palliani & Riding, 1997a); this setting is similar to the Mecsek basin. The characteristic palynological features and the biotic events at these localities are summarised in Table 2.

6.3.1 Comparison with localities from the Northwest European Realm

Marine palynomorphs in the Lower Toarcian of northwest Europe are dominated by *Luehndea spinosa*, *Mancodinium semitabulatum*, *Nannoceratopsis* spp., sphaeromorphs and *Tasmanites* spp. (Bucefalo Palliani & Riding, 1999b, 2003a) similar to the Réka Valley association. In the Yorkshire succession, the dinoflagellate assemblages are gradually replaced by prasinophytes and sphaeromorphs resulting in the dinoflagellate cyst blackout event being coincident with the negative carbon isotope excursion and TOC maximum between the *Dactylioceras semicelatum* and *Harpoceras exaratum* ammonite subbiozones (Bucefalo Palliani et al., 2002). In contrast, in the Réka Valley the replacement of dinoflagellate cysts by prasinophytes was sudden rather than gradual, although it may be attributed to the different

sampling resolution. The length of the phytoplankton disappearance event and the stratigraphical range of the sphaeromorphs are also more extensive in the Hungarian sequence.

In the Posidonia Shale of southwest Germany the relative proportion of *Nannoceratopsis s*e*nex* increases gradually at the top of the *D. tenuicostatum* ammonite biozone to the onset of the bituminous facies, which bears significant resemblance to Interval 2 in the Réka Valley (Table 2). The black shale interval in the Posidonia Shale is also devoid of dinoflagellate cysts, similar to the Interval 3 at Réka Valley. However, in northwest Germany, dinoflagellate cysts (*Nannoceratopsis*) are present throughout the organic-rich facies (Prauss, 1996), explained by the more proximal depostional setting of the Grimmen succession providing refuge for *Nannoceratopsis* with a probably less stable oxygen minmum zone. After the T-OAE the dinoflagellate cysts return only in the upper part of the *H. bifrons* ammonite biozone in southwest Germany (Prauss et al., 1991), but they are less diverse and abundant than before the anoxic period, which is similar to the low phytoplankton diversity and abundance observed in Intervals 4 and 5 in the Réka Valley. Another common feature of the Réka Valley and the assemblages from southwest Germany is the abundance of sporomorphs (pteridophyte spores and bisaccate pollen) together with terrestrial macerals (huminite, vitrinite) in the kerogen in the *P. spinatum* to *D. tenuicostatum* ammonite biozones (Table 2). The replacement of phytoplankton groups and the length of the disappearance event were more pronounced and longer in Germany and in the Réka Valley compared to the Yorkshire section (e.g. Wall, 1965; Prauss & Riegel, 1989; Bucefalo Palliani et al., 2002) (Table 2).

The Quercy succession in southwest France exhibits similar assemblages to those in in northwest Europe or the Réka Valley. *Luehndea spinosa* is dominant in the *D. tenuicostatum* ammonite biozone and the number of species and abundance of *Nannoceratopsis* increased towards the top of that unit (Bucefalo Pallinai & Riding, 1997a). *Nannoceratopsis*

magnicornus was described from this locality, which is also present in the Réka Valley assemblage (Bucefalo Pallinai & Riding, 1997a). The phytoplankton turnover patterns later in the early Toarcian could not be studied in the Quercy succession, as this interval was not exposed there (Bucefalo Pallinai & Riding, 1997a).

6.3.2 Comparison with localities from the Mediterranean Province of the Tethyan Realm

In the Early Jurassic the Mecsek succession was located in a transitional belt between the Mediterraneam areas and the northwest European epicontinental Realm, but it bears a closer resemblance to the latter. For example, *Mendicodinium* spp. are significantly more diverse in the Mediterranean Realm than in the epicontinental areas, whereas *Nannoceratopsis* and *Luehndea* exhibited greater species richness in the latter province (Riding, 1984; Prauss, 1989; Feist-Burkhardt & Wille, 1992). Furthermore, in the early Toarcian not only the assemblages consist of different species, but different patterns of palaeoenvironmental and community changes associated to the T-OAE are present in the two realms (Bucefalo Pallani & Riding, 1999b). The only common features are the extinction of *Luehndea spinosa* before the onset of the black shale deposition in the *D. tenuicostatum* ammonite biozone and the disappearance of dinoflagellate cysts in the organic-rich sediments accompanied by a prasinophyte bloom (Bucefalo Palliani et al. 1998; Bucefalo Pallinai & Riding, 1999 a, b). One of the major differences is the temporal discrepancy between biotic events and community changes in the two provinces. In the Umbria-Marche Basin in Central Italy, the environmental perturbation starts in the lowermost *D. tenuicostatum* ammonite biozone, culminating in the middle-upper part of that zone, and the return of ventilated, oxygenated conditions occurs in the uppermost part of the *D. tenuicostatum* ammonite biozone (Table 2). In the Réka Valley and in the northwest European domain, the onset of the black shale sedimentation and the dinoflagallate cyst disappearance event occur later in the uppermost *D.*

tenuicostatum to *H. falciferum* ammonite biozones and the environmental crisis extends probably into the *H. bifrons* ammonite biozone (Prauss et al. 1991). In the Mediterranean localities no sign of intense terrestrial runoff, freshwater input and freshening of surface waters were recorded, although terrestrial palynomorphs may be abundant at some levels (Bucefalo Palliani, 1997; Bucefalo Palliani & Riding, 1997b). The sphaeromorphs are less significant in the Mediterranean area than in northwest Europe. The palynomorph assemblage of the black shales consists mainly of *Tasmanites* spp. The prasinophyte proliferation may be explained by the intensification of the oxygen minimum zone and the successful nitrogen metabolism of the prasinophytes (Prauss, 2007). Freshening of the surface waters due to riverine influx was not significant in the Tethyan Realm due to the open oceanic settings in Italy (van de Schootbrugge et al., 2013). Moreover after the termination of the black shale depositions, phytoplankton communities recovered rapidly, with new constituents including *Mancodinium semitabulatum, Mendicodinium* spp. and *Susadinium*, which are not present in the coeval assemblages in the upper part of the Réka Valley section (Bucefalo Palliani & Riding, 1999a).

7. Conclusions

The palynological and palynofacies analysis of the lower Toarcian, black shale-bearing Réka Valley section in southwest Hungary clearly demonstrated significant variations in palynomorph groups and sedimentary organic material during the T-OAE environmental perturbation. The organic-walled phytoplankton communities responded to the environmental stress with a multiphase floral disruptions conprising five intervals with gradual reductions in the number of specialist forms in favour of opportunistic taxa. The community replacement was initiated by the climate-driven eutrophication and freshening of the surface waters leading to the blooms of the opportunistic dinoflagellate cyst genus *Luehndea* (Interval 1) and subsequently to to an acme of the euryhaline dinoflagellate cyst genus *Nannoceratopsis*

(Interval 2). The most severe environmental crisis was marked by an interval of prasinophyte abundance (sphaeromorphs and *Tasmanites* spp.) (Interval 3), indicating reduced nutrient sources and altered physico-chemical conditions of the water column due to stratified water column. This biotic crisis was followed by a prolonged recovery period (Intervals 4 and 5). The comparison of the Mediterranean Tethyan and northwest European domains indicates that palaeogeographical setting and regional factors can significantly alter the composition of phytoplankton communities and the turnover patterns including the dynamics and extent of the biotic crisis. The five-stage successive changes observed in the Réka Valley succession are consistent with the community replacement pattern documented in epicontinental areas. By contrast, in the Mediterranean Tethyan Realm, different processes can be traced and there is significant temporal discrepancy between biotic events in the two areas. The proliferation of *Nannoceratopsis* is a regional phenomenon in the Northwest European Realm. It may represent a response to a regional freshening event which is not significant in open oceanic settings and is not a global phenomenon. This event is clearly controlled by climatic factors, as warming induced enhanced continental runoff and intense freshwater input into the marine realms of the epicontinental areas. However, the extinction of the *Luehndea* in the *D. tenuicostatum* ammonite bioone and prasinophyte blooms is recorded both in the Mediterranean and northwest European domains. *Luehndea* did not survive the low surface salinity and oligotrophic conditions established in the surface waters due to the lack of nutrient recirculation in the photic zone. The intensification of oxygen deficiency, oligotrophic conditions and altered availability of trace elements in the seawater all account for the prasinophyte bloom. However, in epicontinental areas the freshening of surface waters by riverine input cannot be neglected and may have played a very important role in supporting the proliferation of this group. These changes are all related to the larger-scale climate-

triggered environmental perturbations that caused changes in the ocean-atmosphere system, oceanic current patterns and the physico-chemical parameters of the seawater.

Acknowledgements

We thank Maria Barbacka (Hungarian Natural History Museum), András Galácz and István Szente (Eötvös Loránd University, Hungary) for their helpful advice during the research. Elzbieta Witkowska (Jagiellonian University, Poland) and Jadwiga Ziaja (W. Szafer Institute of Botany, Polish Academy of Sciences, Poland) are acknowledged for their help with taxonomy and help in collecting the literature. We thank Wolfram M. Kürschner (University of Oslo, Norway) for his constructive comments on the manuscript. Emese Réka Bodor (Hungarian Geological and Geophysical Institute) is thanked for her assistance in the fieldwork and help with data analysis. This research was financed by the Hungarian Scientific Research Fund (project K72633) and the Hantken Miksa Foundation. VB was supported by an AASP Student Scholarship (2013). James B. Riding publishes with the approval of the Executive Director, British Geological Survey (NERC). This is MTM–MTA–ELTE Paleo contribution No. XYZ.

Appendix: Alphabetical list of palynomorphs indentified in the Réka Valley section

Spores

Auritulinasporites triclavis Nilsson 1958

Baculatisporites sp.

Cibotiumspora jurienensis (Balme 1957) Filatoff 1965

Cingutriletes sp.

744*Conbaculatisporites mesozoicus* Klaus 1960

745*Concavisporites toralis* (Leschik 1955) Nilsson 1958

746*Contignisporites problematicus* (Couper 1958) Döring 1965

747*Cyathidites australis* Couper 1953

748*Cyathidites minor* Couper 1953

749*Cyathidites punctatus* (Delcourt & Sprumont 1955) Delcourt et al. 1963

750*Deltoidospora* sp.

751*Dictyophyllidites harrisii* Couper 1958

752*Ischyosporites variegatus* Couper 1958

753*Leptolepidites verrucatus* Couper 1953

754*Lycopodiumsporites* sp.

755*Manumia delcourtii* (Pocock 1970) Dybkjær 1991

756*Neoraistrickia* sp.

757*Osmundacidites wellmanii* Couper 1953

758*Plicifera delicata* (Bolkhovitina 1953) Bolkhovitina 1966

759*Stereisporites* sp.

760*Uvaesporites argenteaeformis* (Bolkhovitina 1953) Schulz 1967

761**Pollen**

762*Alisporites robostus* Nilsson 1958

763*Alisporites* cf. *A. thomasii* (Couper 1958) Nilsson 1958

764*Cerebropollenites* sp.

765*Chasmatosporites elegans* Nilsson 1958

766*Chasmatosporites* sp.

767*Classopollis* sp.

768*Monosulcites minimus* Cookson,1947

769*Monosulcites subgranulosus* Couper 1958

770*Pytiosporites* sp.

771*Spheripollenites psilatus* Couper 1958

772*Vitreisporites pallidus* (Reissinger, 1950) Nilsson 1958

773**Dinoflagellate cysts**

774*Luehndea cirilliae* Bucefalo Palliani et al. 1997

775*Luehndea microreticulata* Bucefalo Palliani et al. 1997

776*Luehndea spinosa* Morgenroth 1970

777*Luehndea* sp.

778*Mancodinium semitabulatum* Morgenroth 1970

779*Mendicodinium* sp.

780*Nannoceratopsis gracilis* Alberti 1961

781*Nannoceratopsis gracilis* subsp. *obsoleta* (Prauss1989) Lentin & Williams 1993

782*Nannoceratopsis magnicornus* Bucefalo Palliani & Riding 1998

783*Nannoceratopsis senex* Van Helden 1977

784*Nannoceratopsis spiculata* Stover 1966

785*Umriadinium mediterraneense* Bucefalo Palliani & Riding 1997

786*Valveodinium* sp.

787**Prasinophytes**

788*Cymathiosphaera pachytheca* Eisenack 1967

789*Leiosphaeridia* sp.

790*Pleurozonaria polyporosa* Mädler 1963

791*Tasmanites* sp.

792**Acritarchs**

793*Baltisphaeridium* sp.

Micrhystridium lymensis Wall 1965

Micrhystridium sp.

Veryhachium sp

References

Adámek, J., 2005. The Jurassic floor of the Bohemian Massif in Moravia – geology and paleogeography. Bulletin of Geosciences, 80, 291–305.

Anderson, D.M., Taylor, C.D., Armbrust, E.V., 1987. The effects of darkness and anaerobiosis on dinoflagellate cyst germination. Limnology and Oceanography, 32, 340-351.

Bailey, T.R., Rosenthal, Y., McArthur, J.M., van de Schootbrugge, B., Thirlwall, M.F., 2003. Paleoceanographic changes of the Late Pliensbachian–Early Toarcian interval: a possible link to the genesis of an Oceanic Anoxic Event. Earth and Planetary Science Letters, 212, 307-320.

Baldanza, A., Bucefalo Palliani, R., Mattioli, E., 1995. Lower Jurassic calcareous nannofossils and dinoflagellate cysts of Hungary and their comparison with assemblages from Central Italy. Palaeopelagos, 5, 161-174.

Bassoulet, J.-P., Elmi, S., Poisson, A., Cecca, F., Bellion, Y., Guiraud, R., Baudin, F., 1993. Middle Toarcian (184-182 Ma.). In: Dercourt, J., Ricou, L. E., Vrielynck, B. (Eds.), Atlas Tethys Paleoenvironmental Maps. BEICIP-FRANLAB, Rueil-Malmaison, pp. 63-80.

Batten, D.J., 2002. Palynofacies and petroleum potential. In: Jansonius, J. & McGregor, D. C. (Eds.), Palynology: Principles and Applications. American Association of Stratigraphic Palynologists Foundation, 1065–1084.

Bleahu, M., Haas, J., Kovács, S., Péró, Cs., Mantea, G., Bordea, S., Ştefănescu, M., Konrád, Gy., Nagy, E., Rálisch-Felgenhauer, Sikić, K., Török, Á., 1994: Triassic facies types,

evolution and paleogeographic relations of the Tisza Megaunit. Acta Geologica Hungarica, 37, 3-4, 187-234.

Branski, P., 2010. Kaolinite peaks in early Toarcian profiles from the Polish Basin - an inferred record of global warming. Geological Quarterly, 54, 15-24.

Bucefalo Palliani, R., 1997. Toarcian sporomorph assemblages from the Umbria-Marche basin, central Italy. Palynology, 21, 105-121.

Bucefalo Palliani, R., Cirilli, S., Mattioli, E., 1998. Phytoplankton response and geochemical evidence of the lower Toarcian relative sea level rise in the Umbria Marche basin (Central Italy). Palaeogeography, Palaeoclimatology, Palaeoecology, 142, 33-50.

Bucefalo Palliani, R., Mattioli, E., Riding, J.B., 2002. The response of marine phytoplankton and sedimentary organic matter to the early Toarcian (Lower Jurassic) oceanic anoxic event in northern England. Marine Micropaleontology, 46, 223-245.

Bucefalo Palliani, R. & Riding, J.B., 1997a. The influence of palaeoenvironmental change on dinoflagellate cyst distribution. An example from the lower and middle Jurassic of Quercy, Southwest France. Bulletin du Centre de Recherches Elf Exploration-Production, 21, 107-123.

Bucefalo Palliani, R. & Riding, J.B., 1997b. Lower Toarcian palynostratigraphy of Pozzale, central Italy. Palynology, 21, 91-103.

Bucefalo Palliani, R. & Riding, J.B., 1999a. Relationship between the early Toarcian anoxic event and organic-walled phytoplankton in central Italy. Marine Micropaleontology, 37, 101-116.

Bucefalo Palliani, R. & Riding, J.B., 1999b. Early Jurassic (Pliesnbachian-Toarcian) dinoflagellate migrations and cyst paleoecology in the Boreal and Tethyan realms. Micropaleontology, 45, 201-214.

Bucefalo Palliani, R. & Riding, J.B., 2000. A palynological investigation of the Lower and lowermost Middle Jurassic strata (Sinemurian to Aalenian) from North Yorkshire, UK. Proceedings of the Yorkshire Geological Society, 53, 1-16.

Bucefalo Palliani, R. & Riding, J.B., 2003a. Biostratigraphy, provincialism and evolution of European early Jurassic (Pliensbachian to early Toarcian) dinoflagellate cysts. Palynology, 27, 179-214.

Bucefalo Palliani, R. & Riding, J.B., 2003b. Umbriadinium and Polarella: an example of selectivity in the dinoflagellate fossil record. Grana, 42, 108-111.

Bucefalo Palliani, R., Riding, J.B., Torricelli, S., 1997. The dinoflagellate cyst Luehndea Morgenroth, 1970, emend. from the upper Pliensbachian (Lower Jurassic) of Hungary. Review of Palaeobotany and Palynology, 96, 113-120.

Burgess, S.D., Bowring, S.A., Fleming, T.H., Elliot, D.H., 2015. High-precision geochronology links the Ferrar large igneous province with early-Jurassic ocean anoxia and biotic crisis. Earth and Planetary Science Letters 415, 90–99.

Caruthers, A.H., Smith, P., Gröcke, D.R., 2013. The Pliensbachian–Toarcian (Early Jurassic) extinction, a global multi-phased event. Palaeogeography, Palaeoclimatology, Palaeoecology, 386, 104-118.

Caswell, B.A. & Coe, A.L., 2013. Primary productivity controls on opportunistic bivalves during Early Jurassic oceanic deoxygenation. Geology, 41, 1163-1166.

Correa-Metrio, A., Dechnik, Y., Socorro, L.-G., Caballero, M., 2014. Detrended correspondence analysis: A useful tool to quantify ecological changes from fossil data set. Boletín de la Sociedad Geológica Mexicana, 66, 135-143.

Császár, G., Görög, Á., Gyuricza, Gy., Sieglné Farkas, Á., Szente, I., Szinger, B., 2007. The geological, palaeontological and sedimentological pattern of the Vasa Marl Formation

between Zsibrik and Ófalu, South Transdanubia. Földtani Közlöny, 137, 193–226 `(in Hungarian with English abstract)`

Csontos, L., Benkovics, L., Bergerat, F., Mansy, J., Wórum, G., 2002. Tertiary deformation history from seismic section study and fault analysis in a former European Tethyan margin (the Mecsek–Villány area, SW Hungary). Tectonophysics, 357, 81–102.

Csontos, L., Nagymarosy, A., Horváth, F., Kovác, M., 1992. Tertiary evolution of the Intra-Carpathian area: a model. Tectonophysics, 208, 221–241.

Csontos, L. & Vörös, A., 2004. Mesozoic plate tectonic reconstruction of the Carpathian region. Palaeogeography, Palaeoclimatology, Palaeoecology, 210, 1–56.

Danise, S., Twitchett, R.J., Little, T.S., Clémance, M.-E., 2013. The impact of global warming and anoxia on marine benthic community dynamics: an example from the Toarcian (Early Jurassic). PLOS ONE, 8, e56255.

Davies, E.H., 1985. The miospore and dinoflagellate cyst Oppel-zonation of the Lias of Portugal. Palynology, 9, 105-132.

Dera, G., Pellenard, P., Neige, P., Deconinck, J.-F., Pucéat, E., Dommergues, J.-L., 2009. Distribution of clay minerals in Early Jurassic Peritethyan seas: Palaeoclimatic significance inferred from multiproxy comparisons. Palaeogeography, Palaeoclimatology, Palaeoecology, 271, 39-51.

De Toledo, M.B., Barth, O.M., Silva, C.G., Barros, M.A., 2009. Testing multivariate analysis in paleoenvironmental reconstructions using pollen records from Lagoa Salgada, NE Rio de Janeiro State, Brazil. Annals of the Brazilian Academy of Sciences, 81, 757-768.

Dulai, A., Suba, Z., Szarka, A., 1992. Toarcian (Lower Jurassic) organic-rich black shale in the Réka valley (Mecsek Hills, Hungary). Földtani Közlöny, 122, 67-87.

889Dybkjær, K., 1991. Palynological zonation and palynofacies of the Fjerritslev Formation
890 (Lower Jurassic–basal Middle Jurassic) in the Danish Subbasin. Geol. Surv. Denmark,
891 DGU Series A, 30, 1–150.
892Ellegard, M., 2000. Variations in dinoflagellate cyst morphology under conditions of changing
893 salinity during the last 2000 years in the Limfjord, Denmark. Review of Palaeobotany
894 and Palynology, 109, 65-81.
895Erba, E., 2004: Calcareous nannofossils and Mesozoic oceanic anoxic events. Marine
896 Micropaleontology, 52, 85-106.
897Evitt, W.R., 1961. The dinoflagellate *Nannoceratopsis* Deflandre; morphology, affinities and
898 infraspecific variability. Micropaleontology, 7, 305-316.
899Falkowski, P.G., Katz, M.E.,Knoll, A.H.,Quigg, A., Raven, J.A., Schofield, O., Taylor, F.J.R.,
900 2004. The evolution of modern eukaryotic phytoplankton. Science, 305, 354–360.
901Farrimond, P., Eglinton, G., Brassell, S.C., Jenkyns, H.C., 1989. Toarcian anoxic event in
902 Europe: An organic geochemical study. Marine and Petroleum Geology, 6, 136-147.
903Feist-Burkhardt, S., Götz, A., Ruckwied, K., Russel, J., 2008. Palynofacies patterns,acritarch
904 diversity and stable isotope signatures in the Lower Muschelkalk (Middle Triassic) of N
905 Switzerland: Evidence of third-order cyclicity. Swiss Journal of Geosciences, 101, 1-15.
906Feist-Burkhardt, S. & Wille, W., 1992. Jurassic palynology in southwest Germany – state of
907 the art. Cahiers de Micropaléontologie, 7, 141-164.
908Fensome, R.A., Taylor, F.J.R., Norris, G., Sarjeant, W.A.S., Wharton, D.I.,Williams, G.L.,
909 1993. A classification of living and fossil dinoflagellates, American Museum of Natural
910 History, New York
911Galácz, A., 1991: Palaeontological investigation of the Toarcian black shale in the Mecsek
912 Mts. Unpublished manuscript, Department of Palaeontology, Eötvös Loránd University,
913 pp. 1-32. `(in Hungarian)`

914Gocht, H., 1964. Planktonische Kleinformen aus dem Lias-/Dogger-Grenzbereich Nord- und
915 Süddeutschlands. Neues Jahrbuch für Gelogie und Paläontologie Abhandlungen, 119,
916 113-133.
917Gocht, H., 1972. Zur Morphologie der Dinoflagellaten-Gattung Nannoceratopsis Deflandre.
918 Lethaia, 5, 15-29.
919Götz, A. E., Feist-Burkhardt, S., Ruckwied, K., 2008. Palynofacies and sea-level changes in
920 the Upper Cretaceous of the Vocontian Basin, southeast France. Cretaceous Research,
921 29, 1047-1057.
922Grimm, E.C., 1987. CONISS: a FORTRAN 77 program for stratigraphically constrained
923 cluster analysis by the method of incremental sum of squares. Computers &
924 Geosciences 13, 13–35.
925Grimm, E.C., 1991–2001. Tilia, TiliaGraph and TGView Software, Illinois State Museum,
926 Springfield, Illinois, USA.
927Guy-Ohlson, D., 1986: Jurassic palynology of the Vilhelmsfalt bore no.1, Scania, Sweden:
928 Toarcian-Aalenian. Stockholm, Section of Palaeobotany Swedish Museum of Natural
929 History, 127 p.
930Haas, J. & Péró, Cs., 2004. Mesozoic evolution of the Tisza Mega-unit. International Journal
931 of Earth Sciences, 93, 297-313.
932Hammer, Ø., Harper, D.A.T., Ryan, P.D., 2001. PAST: palaeontological statistics software
933 package for education and data analysis. Palaeontologica Electronica, 4, 9.
934Harries, P.J. & Little, C.T.S., 1999. The early Toarcian (Early Jurassic) and the Cenomanian–
935 Turonian (Late Cretaceous) mass extinctions: similarities and contrasts.
936 Palaeogeography, Palaeoclimatology, Palaeoecology 154, 39-66.
937Hermoso, M., Minoletti, F., Pellenard, P., 2013. Black shale deposition during Toarcian super-
938 greenhouse driven by sea level. Climate of the Past, 9, 2703-2712.

939Hesselbo, S.P., Gröcke, D.R, Jenkyns, H.C, Bjerrum, C.J., Farrimond, P., Green, O.R., 2000.
940 Massive dissociation of gas hydrate during a Jurassic oceanic anoxic event, Nature, 406,
941 392-395.
942Hesselbo, S.P., Jenkyns, H.C., Duarte, L.V., Oliveira, L.C.V., 2007. Carbon-isotope record of
943 the Early Jurassic (Toarcian) Oceanic Anoxic Event from fossil wood and marine
944 carbonate (Lusitanian Basin, Portugal). Earth and Planetary Science Letters, 253, 455-
945 470.
946Hill, M.O. & Gauch, H.G., 1980. Detrended correspondence analysis: an improved ordination
947 technique. Vegetatio, 42, 47-58.
948Horváth, F. & Galácz, A., 2006. The Carpathian-Pannonian Region. A Review of Mesozoic-
949 Cenozoic Stratigraphy and Tectonics. Hantken Press, Budapest, pp. 1-624.
950Jenkyns, H.C., 1988. The early Toarcian (Jurassic) anoxic event; stratigraphic, sedimentary
951 and geochemical evidence. American Journal of Science, 288, 101-151.
952Jenkyns, H.C., Gröcke, D.R., Hesselbo, S.P., 2001. Nitrogen isotope evidence for water mass
953 denitrification during the early Toarcian (Jurassic) oceanic anoxic event.
954 Paleoceanography, 16, 1–11.
955Jenkyns, H.C., Jones, C.E., A Gröcke, D.R., Hesselbo, S.P., Parkinson, D.N., 2002.
956 Chemostratigraphy of the Jurassic System: applications, limitations and implications for
957 palaeoceanography. Journal of the Geological Society, 159, 351-378.
958Katz, M.E., Finkel, Z.V., Grzebyk, D., Knoll, A.H., Falkowski, P.G., 2004. Evolutionary
959 trajectories and biochemical impacts of marine eukaryotic phytoplankton. Annu. Rev.
960 Ecol. Evol. Syst. 35, 523–56.
961Korte, C. & Hesselbo, S.P., 2011. Shallow marine carbon and oxygen isotope and elemental
962 records indicate icehouse-greenhouse cycles during the Early Jurassic.
963 Paleoceanography,26, PA4219.

964Legendre, P. & Legendre, L., 1998. Numerical Ecology. Elsevier Scientific, Oxford, United
965 Kingdom.
966
967Littler, K., Hesselbo, S.P., Jenkyns, H.C., 2009. A carbon-isotope perturbation at the
968 Pliensbachian–Toarcian boundary: evidence from the Lias Group, NE England,
969 Geological Magazine, 147, 181–192.
970Loh, H., Maul, B., Prauss, M., Riegel, W., 1986. Primary production, maceral formation and
971 carbonate species in the Posidonia Shale of NW Germany. In: Degens, E. T., Meyers, P.
972 A., Brassel, S. C. (Eds.), Biogeochemistry of black shales. Mitt. Geol. Paläont. Inst.
973 Univ. Hamburg, 60, pp. 397-421.
974Lund, J.J. & Pedersen, K.R., 1984. Palynology of the marine Jurassic formations in the
975 Vardekløft ravine, Jameson Land, East Greenland. Bulletin of the Geological Society of
976 Denmark 33, 371-400.
977Marret, F. & Zonneveld, K., 2003. Atlas of modern organic-walled dinoflagellate cyst
978 distribution. Review of Palaeobotany and Palynology 125, 1–200.
979Mattioli, E. & Erba, E., 1999. Synthesis of calcareous nannofossil events in Tethyan Lower
980 and Middle Jurassic succesions. Rivista Italiana di Paleontologia e Stratigrafia, 105,
981 343-376.
982Mattioli, E., Pittet, B., Bucefalo Palliani, R., Röhl, H.-J., Schmid- Röhl, A., Morettini, E.,
983 2004. Phytoplankton evidence for the timing and correlation of palaeoceanographical
984 changes during the early Toarcian oceanic anoxic event (Early Jurassic). Journal of the
985 Geological Society, 164, 685-693.
986Mattioli, E., Pittet, B., Petitpierre, L., Maillot, S., 2009. Dramatic decrease of pelagic
987 carbonate production by nannoplankton across the Early Toarcian anoxic event (TOAE).
988 Global and Planetary Change, 65, 134-145.
989McArthur, J.M., Donovan, D.T., Thirlwall, M.F., Fouke, B.W., Mattey, D., 2000. Strontium
990 isotope profile of the early Toarcian (Jurassic) oceanic anoxic event, the duration of

ammonite biozones, and belemnite palaeotemperatures. Earth and Planetary Science Letters, 179, 269-285.

McElwain, J.C., Wade-Murphy, J., Hesselbo, S.P., 2005. Changes in carbon dioxide during an oceanic anoxic event linked to intrusion into Gondwana coals. Nature, 435, 479-82.

Mertens, K.N., Bradley, L.R., Takano, Y., Mudie, P.J., Marret, F., Aksu, A.E., Hiscott, R.N., Verleye, T.J., Mousing, E.A., Smyrnova, L., Bagheri, S., Mansor, M., Pospelova, V., Matsuoka, K., 2012. Quantitative estimation of Holocene surface salinity variation in the Black Sea using dinoflagellate cyst process length. Quaternary Science Reviews, 39, 45-59.

Némedi Varga, Z.,1998. Jurassic lithostratigraphy of the Mecsek and Villany. In: Bérczi, I., Jámbor, Á. (Eds.), Lithostratigraphic units in Hungary. MOL Hun. Oil Gas Comp. and Geological Institute of Hungary, Budapest, pp. 319–336. `(in Hungarian)`

Oboh-Ikuenobe, F. E & de Villiers, S.E., 2003. Dispersed organic matter in samples from the western continental shelf of Southern Africa: palynofacies assemblages and depositional environments of Late Cretaceous and younger sediments. Palaeogeography, Palaeoclimatology, Palaeoecology 201, 67-88.

Pálfy, J. & Smith, P. L., 2000. Synchrony between Early Jurassic extinction, oceanic anoxic event, and the Karoo-Ferrar flood basalt volcanism. Geology, 28, 747-750.

Pittet, B. & Gorin, G.E., 1997. Distribution of sedimentary organic matter in a mixed carbonate-siliciclastic platform environment: Oxfordian of the Jura Mountains. Sedimentology 44, 915-937.

Prauss, M., 1989. Dinozysten-Stratigraphie und Palynofazies im Oberen Lias und Dogger von NW-Deutschland. Palaeontographica Abt. B, 214, 1-124.

Prauss, M., 1996. The Lower Toarcian Posidonia Shale of Grimmen, northwest Germany. Neues Jahrb. Geol. Palaäontol. Abh., 200, 107-132.

1016Prauss, M., 2007. Availability of reduced nitrogene chemospecies in photic-zone waters as the
1017 ultimate cause for fossil prasinophyte prosperity. Palaios, 22, 489-499.
1018Prauss, M., Ligouis, B., Lutbacher, H.-P., 1991. Organic matter and palynomorphs in the
1019 ‘‘Posidonienschiefer’’ (Toarcian, Lower Jurassic) of southern Germany. In: Tyson, R. V.
1020 & Pearson, T.H. (Eds), Modern and Ancient Continental Shelf Anoxia, Geological
1021 Society Special Publications, London, 58, pp. 335–351.
1022Prauss, M. & Riegel, W., 1989. Evidence from phytoplankton associations for causes of
1023 blackshale formation in epicontinental seas. Neues Jahrbuch für Geologie,
1024 Paläontologie, Monatshefte, 11, 671-682.
1025Pross, J.**,** 2001. Paleo-oxygenation in Tertiary epeiric seas: Evidence from dinoflagellate cysts.
1026 Palaeogeography, Palaeoclimatology, Palaeoecology, 166, 369-381.
1027Raucsik, B., 2008. Apátvarasd, Réka Valley, opposite to the Disznós Spring, black shale
1028 outcrop. In: Galácz, A.,Konrád, Gy., Raucsik, B.,Vörös, A. 2008 (Eds.), Jurassic
1029 siliciclastics and carbonates of the Mecsek-Villány area. Field Trip Guide of the
1030 geological excursion on the Mecsek and Villány Hills Organized by the Hungarian
1031 Geological Society and the Sedimentological Subcommission of the Hungarian
1032 Academy of Sciences, 33-37.
1033Raucsik, B., 2012a. Vasas Marl Formation. In: Főzy, I. (Ed.), Jurassic lithostratigrpahic units
1034 in Hungary. Hungarian Geological Society, pp. 152-154. ‘(in Hungarian)’
1035Raucsik, B., 2012b. Hosszúhetény Calcareous Marl Formation. In: Főzy, I. (Ed.), Jurassic
1036 lithostratigrpahic units in Hungary. Hungarian Geological Society, pp. 155-158. ‘(in
1037 Hungarian)’
1038Raucsik, B., 2012c. Rékavölgy Siltstone Formation. In: Főzy, I. (Ed.), Jurassic
1039 lithostratigrpahic units in Hungary. Hungarian Geological Society, pp. 164-167. ‘(in
1040 Hungarian)’

Raucsik, B., 2012d. Komló Calcareous Marl Formation. In: Főzy, I. (Ed.), Jurassic lithostratigraphic units in Hungary. Hungarian Geological Society, pp. 174—176. ‘(in Hungarian)’

Raucsik, B. & Varga, A., 2008a. Climato-environmental controls on clay mineralogy of the Hettangian–Bajocian successions of the Mecsek Mountains, Hungary: An evidence for extreme continental weathering during the early Toarcian oceanic anoxic event. Palaeogeography, Palaeoclimatology, Palaeoecology, 265, 1-13.

Raucsik, B. & Varga, A., 2008b. Mineralogy of the Lower Toarcian black shale section from the Réka Valley (Óbánya Siltstone Formation, Mecsek Mountains, Hungary): implications for palaeoclimate. Földtani Közlöny, 138, 133-146. (in Hungarian with English abstract).

Riding, J.B., 1983. The palynology of the Aalenian (Middle Jurassic) sediments of Jackdaw Quarry, Gloucestershire, England. Mercian Geologist, 9, 111–120.

Riding, J.B., 1984. A palynological investigation of Toarcian to early Aalenian strata from the Blea Wyke area, Ravenscar, North Yorkshire. Proc. Yorkshire Geol. Soc, 45, 109-122.

Riding, J.B., 1985. Dinoflagellate cyst range-top biostratigraphy of the Uppermost Triassic to Lowermost Cretaceous of northwest Europe. Palynology, 8, 195-210.

Riding, J.B., 1987. Dinoflagellate cyst stratigraphy of the Nettleton Bottom Borehole (Jurassic: Hettangian to Kimmeridgian) Lincolnshire, England. Proceedings of the Yorkshire Geological Society, 46, 231-266.

Riding, J.B. & Thomas, J.E., 1992: Dinoflagellate cysts of the Jurassic System. In: Powell, A. J. 1992 (Ed.): A stratigraphic index of dinoflagellate cysts, British Micropalaeontological Society Publications Series, pp. 7-97.

1064Rochon, A., Lewis, J., Ellegaard, M., Harding, I.C., 2009. The *Gonyaulax spinifera*
1065 (Dinophyceae) “complex”: Perpetuating the paradox? Review of Palaeobotany and
1066 Palynology, 155, 52–60.
1067Röhl, H.-J. & Schmid-Röhl, A., 2005. Lower Toarcian (Upper Liassic) black shales of the
1068 Central European epicontinental basin: a sequence stratigraphic case study from the SW
1069 Germany, Posidonia Shale. SEPM Special Publications, 82, 165–189.
1070Schouten, S., van Kaam-Peters, H.M.E., Rijpstra, W.I.C., Schoell, M., Sinnighe Damaste, J.S.,
1071 2000. Effects of an anoxic event on the stable carbon isotope composition of Early
1072 Toarcian carbon. American Journal of Science, 300, 1-22.
1073Stover, L.E., Brinkhuis, H., Damassa, S.P., De Verteuil, L, Helby, R.J., Monteil, E., Partridge,
1074 A.D., Powell, A.J., Riding, J.B., Smelror, M., Williams, G.L., 1996. Mesozoic-Tertiary
1075 dinoflagellates, acritarchs and prasinophytes. In: Jansonius, J. & McGregor, D. C. (Eds),
1076 Palynology: principles and applications, AASP Foundation, 2, pp. 641-750.
1077Suan, G., Mattioli, E., Pittet, B., Maillot, S., Lécuyer, C., 2008. Evidence for major
1078 environmental perturbation prior to and during the Toarcian (Early Jurassic) oceanic
1079 anoxic event from the Lusitanian Basin, Portugal. Paleoceanography, 23, PA1202.
1080Svensen, H., Planke, S., Chevallier, L., Malthe-Sørenssen, A., Corfu, F., Jamtveit, B., 2007.
1081 Hydrothermal venting of greenhouse gases triggering Early Jurassic global warming.
1082 Earth and Planetary Science Letters, 256, 554-566.
1083Szente, I. 2012. Mecsek Coal Formation. In: Főzy, I. (Ed.), Jurassic lithostratigraphic units in
1084 Hungary. Hungarian Geological Society, Budapest, pp. 145-148. ‘(in Hungarian)’
1085Tyson, R.V., 1993. Chapter 5: Palynofacies analysis. In: Jenkins, D. G. (Ed.) Applied
1086 Micropaleontology. Kluwer Academic Publishers, The Netherlands, Amsterdam, pp.
1087 153-191.

1088Tyson, R.V., 1995. Sedimentary organic matter Organic facies and palynofacies. Chapman &
1089 Hall, London
1090van de Schootbrugge, B., Bachan, A., Suan,. G., Richoz, S., Payne, J., 2013. Microbes, mud
1091 and methane: cause and consequence of recurrent Early Jurassic anoxia following the
1092 end-Triassic mass extinction. Palaeontology, pala.12034, pp. 1-25.
1093van de Schootbrugge, B., Mcarthur, J.M., Bailey, T.R., Rosenthal, Y., Wright, J.D., Miller,
1094 K.G., 2005a. Toarcian oceanic anoxic event: assessment of global causes using
1095 belemnite C-isotope records. Paleoceanography, 20, PA3008.
1096van de Schootbrugge, B., Bailey, T.R., Rosenthal, Y., Katz, M.E., Wright, J.D., Miller, K.G.,
1097 Feist-Burkhardt, S., Falkowski P.G., 2005b: Early Jurassic climate change and the
1098 radiation of organic-walled phytoplankton in the Tethys Ocean. Paleobiology, 31, 73-97.
1099van de Schootbrugge, B, Quan, T.M., Lindström, S., Püttmann, W., Heunisch, C., Pross, J.,
1100 Fiebig, J., Petschick, R., Röhling, H., Richoz, H.-G., Rosenthal, Y., Falkowski, P.G.
1101 2009. Floral changes across the Triassic–Jurassic boundary linked to flood basalt
1102 volcanism. Nature Geoscience, 2, 589–594.
1103van Erve, A.W., 1977. Palynological investigation in the Lower Jurassic of the Vicentinian
1104 Alps (Northeastern Italy). Review of Palaeobotany and Palynology 23, 1-117.
1105Varga, A., Mikes, T., Raucsik, B. 2009: The petrography and heavy minerals of the Toarcian
1106 black shale of the Réka Valley section of the Mecsek Hills: a pilot study. Földtani
1107 Közlöny, 139, 31-53. `(in Hungarian with English abstract)`
1108Varga, A.R., Raucsik, B., Hámor-Vidó, M., Rostási, A., 2007. Isotope geochemistry and
1109 characterization of hydrocarbon potential of black shale from Óbánya Siltstone
1110 Formation. Földtani Közlöny, 137, 449–472. `(in Hungarian with English abstract)`
1111Verleye, T.J., Mertens, K.N., Young, M.D., Dale, B., McMinn, A., Scott, L., Zonneveld,
1112 K.A.F., Louwye, S., 2012. Average process length variation of the marine dinoflagellate

cyst *Operculodinium centrocarpum* in the tropical and Southern Hemisphere Oceans: Assessing its potential as a palaeosalinity proxy. Marine Micropaleontology, 86–87, 45–58.

Wall, D., 1965. Microplankton, pollen, and spores from the Lower Jurassic in Britain. Micropaleontology, 11, 151-190.

Wignall, P.B., 2001. Large igneous provinces and mass extinctions. Earth-Science Reviews 53, 1–33.

Wignall, P.B. & Benton, M.J., 1999. Lazarus taxa and fossil abundances at times of biotic crisis. Journal of the Geological Society of London 156, 453-456.

Wille, W., 1982. Ecology and evolution of upper Liassic dinoflagellates from SW Germany. Neues Jahrbuch für Geologie und Paläontolgie, Abhandlungen, 164, 74-82.

Wood, G.D., Gabriel, A.M., Lawson, J.C., 1996. Palynological techniques – processing and microscopy. In: Jansonius, J. & McGregor, D. C. (Eds), Palynology: Principles and applications: AASP Foundation, Dallas, 1, pp. 29-50.

Figure captions

Figure 1. A. The geological framework and major tectonic units of the Carpathian–Pannonian area (after Csontos & Vörös, 2004). The box indicates the area shown in Fig. 1B. B. Generalised geological map of the Mecsek Mountains showing the distribution of Jurassic strata. The location of the Réka Valley section is marked by an asterisk. Modified after Raucsik & Varga (2008a), with structural geology from Csontos et al. (2002).

Figure 2. The Early Jurassic palaeogeography of the western Neotethys and adjacent epicontinental areas, showing the position of the area studied and the other occurrences of

1137Lower Toarcian black shales discussed in the text (Jenkyns, 1988). Modified after Varga et al.
1138(2007); base map after Bassoulet et al. (1993).
1139
1140Figure 3. The lithostratigraphy of the Lower and Middle Jurassic formations of the Mecsek
1141Mountains indicating their depositional settings; modified after Raucsik & Varga (2008a).
1142Figure 4. Location map of the section investigated (above) and a closeup photograph of the
1143outcrop (below). Key: 1 – creek; 2 – trail; 3 – road; 4 – settlement. Modified after Raucsik &
1144Varga (2008b).
1145
1146Figure 5. A. Lithological log of the Réka Valley section with the palynomorph samples,
1147modified after Galácz (1991). B. Detailed lithological log of the black shale interval, modified
1148after Raucsik & Varga (2008b) and Varga et al. (2009).
1149
1150Figure 6. The Simpson Diversity Index and the relative proportions of different palynomorph
1151groups in the Réka Valley section. The abundance of palynomorphs is given in percentages.
1152The group “Other dinoflagellate cysts” includes *Mancodinium semitabulatum*,
1153*Mendicodinium* sp., *Valveodinium* sp. and *Umbriadinium mediterranense*; the low abundances
1154of these forms does not permit to the separate plotting of them. The lithological log on the left
1155is not to scale. The area in grey shading has an exaggeration factor of X2.
1156
1157Figure 7. Palynofacies results and values of the different palynofacies indicesin the studied
1158section. The indices were not calculated for the samples from the black shale interval because
1159of the overwhelming dominance of amorphous organic matter (AOM) that hindered the
1160counting of any other organic particles. The following palynofacies indices are shown: ratio of
1161terrestrial to marine palynomorphs (t/m); ratio of spores to bisaccate pollen grains (sp/bs);

ratio of opaque to translucent phytoclasts (o/t); ratio of bladded-lath shaped to equidimensional opaque phytoclasts (bl/eq). The lithological log on the left was not drawn to scale.

Figure 8. Scatter plot of detrended correspondence analysis (DCA) performed on the samples from Réka Valley to detect palaeoecological signals in the palynomorph assemblages.

Table 1. Summary of the palynofacies terminology and the different palynofacies indices. The terminology used is that of Oboh-Ikuenobe & de Villiers (2003), Feist-Burkhardt et al. (2008) and Götz et al. (2008).

Table 2. A comparison of the palynomorph records and biotic events from five localities, including the Réka Valley section. Based on data from Prauss (1989; 1996; 2007), Prauss et al. (1991), Bucefalo Palliani & Riding (1997a; 1999a) and Bucefalo Palliani et al. (1998; 2002).

Plate I. Dinoflagellate cysts from the Réka Valley section. The scale bar represents 20 µm. The sample number and the slide number are given after the taxon name, e.g. RV 10/1.

1. *Nannoceratopsis senex* Van Helden 1977 [RV 10/1].
2. *Nannoceratopsis gracilis* Alberti 1961 [RV 8/2].
3. *Nannoceratopsis gracilis* Alberti 1961 [RV 9/2]
4. *Nannoceratopsis gracilis* subsp. *obsoleta* (Prauss 1989) Lentin & Williams 1993 [RV 8/1].
5. *Nannoceratopsis gracilis* subsp. *obsoleta* (Prauss 1989) Lentin & Williams 1993 [RV 8/1].
6. *Nannoceratopsis* sp. [RV 9/2].
7. *Nannoceratopsis gracilis* Alberti 1961 [RV 9/2]
8. *Nannoceratopsis gracilis* Alberti 1961[RV 2/1]
9. *Luehndea microreticulata* Bucefalo Palliani et al. 1997 [RV 4/1].
10. *Luehndea microreticulata* Bucefalo Palliani et al. 1997 [RV 4/2].

11. *Nannoceratopsis* cf. *N. magnicornus* Bucefalo Palliani & Riding 1997 [RV 8/1].
12. *Luehndea spinosa* Morgenroth 1970 [RV 9/1].
13. *Nannoceratopsis spiculata* Stover 1966 [RV 20/1].

Plate II. Pollen and spores from the Réka Valley section. The scale bar represents 20 µm unless otherwise indicated. The sample number and the slide number are given after the taxon name, e.g. RV 10/1.

1. *Contignisporites problematicus* (Couper 1953) Döring 1965 [RV 11/2].
2. *Ischyosporites variegatus* Couper 1958 [RV 11/2].
3. *Cingutriletes* sp. [RV 18/1].
4. *Cibotiumspora jurienensis* (Balme 1957) Filatoff 1965 [RV 11/2].
5. *Dictyophyllidites harrisii* Couper 1958 [RV 11/2].
6. *Auritulinasporites triclavis* Nilsson 1958 [RV 8/2].
7. *Cyathidites australis* Couper 1953 [RV 4/1]; scalebar = 30 µm.
8. *Neoraistrickia* sp. [RV 16/1].
9. *Osmundacidites wellmanii* Couper 1953 [RV 11/1].
10. *Manumia delcourtii* (Pocock 1970) Dybkjær 1991 [RV 16/1].
11. *Baculatisporites* sp. [RV 8/2].
12. *Concavisporites toralis* (Leschik 1955) Nilsson 1958 [RV 3/1].
13. *Classopollis* sp. [RV 7/1].
14. *Alisporites robostus* Nilsson 1958 [RV 1/1]; scalebar = 30 µm.
15. *Spheripollenites psilatus* Couper 1958 [RV 13/1]; scalebar = 50 µm.
16. *Classopollis* sp. [RV 3/2].
17. *Alisporites* cf. *A. thomasii* (Couper 1958) Nilsson 1958 [RV 4/2].
18. *Chasmatosporites* sp. [RV 3/2].
19. *Monosulcites minimus* Cookson 1947 [RV 3/2].

Plate III. Sphaeromorphs and palynofacies from the Réka Valley section.

1. Sphaeromorphs in clusters. Sample BS 32; scalebar = 20 µm.
2. Sphaeromorphs in clusters. Sample BS 56; scalebar = 20 µm.
3. Fluorescence photomicrograph of amorphous organic material (AOM). The particles with higher fluorescence intensities are palynomorphs and the phytoclasts are masked by AOM; scalebar = 50 µm.
4. Palynofacies of Assemblage 3 with predominant AOM; scalebar = 100 µm.

5. Palynofacies of Assemblage 1 with predominant translucent phytoclasts; scalebar = 100 µm.
6. Palynofacies of Interval 2 with *Nannoceratopsis* sp. from Plate I, fig. 6; scalebar = 100 µm.
7. Palynofacies of Interval 4 with high levels of translucent phytoclasts; scalebar = 100 µm.
8. Palynofacies of Interval 5 with predominant opaque, equidimensional phytoclasts; scalebar = 100 µm.

Supplementary material

Data_sheet.xls contains the palynomorph counts and the calculated playnofacies indices
DCA_samples.xls contains the data set used in the DCA analysis

Major palaeoenvironmental and palaeoceanographic changes occurred during the late Pliensbachian to early Toarcian (Early Jurassic) leading to the Toarcian Oceanic Anoxic Event (T-OAE) and the perturbation of the global carbon cycle that seriously affected marine ecosystems. The sequence of successive steps of environmental change and regional differences in the unfolding of T-OAE are not yet fully understood, and organic-walled phytoplankton and other palynomorphs are well-suited but underexplored for such studies. Based on the quantitative palynological analyses of thirty-three samples from a black shale-bearing succession in the Réka Valley, Mecsek Mountains, southwest Hungary, five distinctive assemblages are distinguished. These define major shifts in the organic-walled phytoplankton communities and were driven by palaeoenvironmental changes. Palynofacies analysis was also carried out in order to detect changes in the composition of sedimentary organic matter and estimate the terrestrial input.

The lowermost Assemblage 1 is characterized by a moderately diverse phytoplankton community and high levels of terrestrial palynomorphs. In Assemblage 2 a significant peak of the euryhaline dinoflagellate cyst *Nannoceratopsis* is present. This is followed by a dominance of highly opportunistic prasinophytes, coinciding with the temporary disappearance of all dinoflagellate cyst taxa (Assemblage 3). This phytoplankton crisis was followed by a prolonged repopulation phase with low diversity phytoplankton assemblages (Assemblages 4 and 5) and intermittently high levels of terrestrially-derived palynomorphs.

The successive disappearance of individual phytoplankton taxa and the gradual takeover by opportunistic euryhaline species at the onset of the early Toarcian environmental perturbations were related to the establishment of a reduced salinity layer in the surface water, a stable pycnocline and deterioration of nutrient recycling followed by oxygen deficiency in the water column. The palaeoenvironmental shifts were driven by early Toarcian global warming, which enhanced the hydrological cycle leading to intense runoff and freshwater input into the

sedimentary basin of the Mecsek Mountains as evidenced by the high amount of terrestrially-derived palynodebris in the palynofacies.

Comparison with coeval European successions reveals that the palaeoenvironmental changes during the T-OAE were not entirely synchronous, and local factors played a crucial role in influencing phytoplankton communities. Because the Réka Valley section was located in the northwest European epicontinental realm during the Early Jurassic, regional freshening of the surface waters and increased terrestrial input due to the proximity of the hinterland had a greater influence on phytoplankton communities compared to the open oceanic setting of the Tethyan Realm.

Detailed quantitative palynological analysis of a Toarcian black shale succession

Five intervals record successive changes in organic-walled phytoplankton assemblages

Peak of the euryhaline genus *Nannoceratopsis*, followed by a dinoflagellate cyst disappearance event

Changes driven by global warming, enhanced runoff, and freshening of surface waters

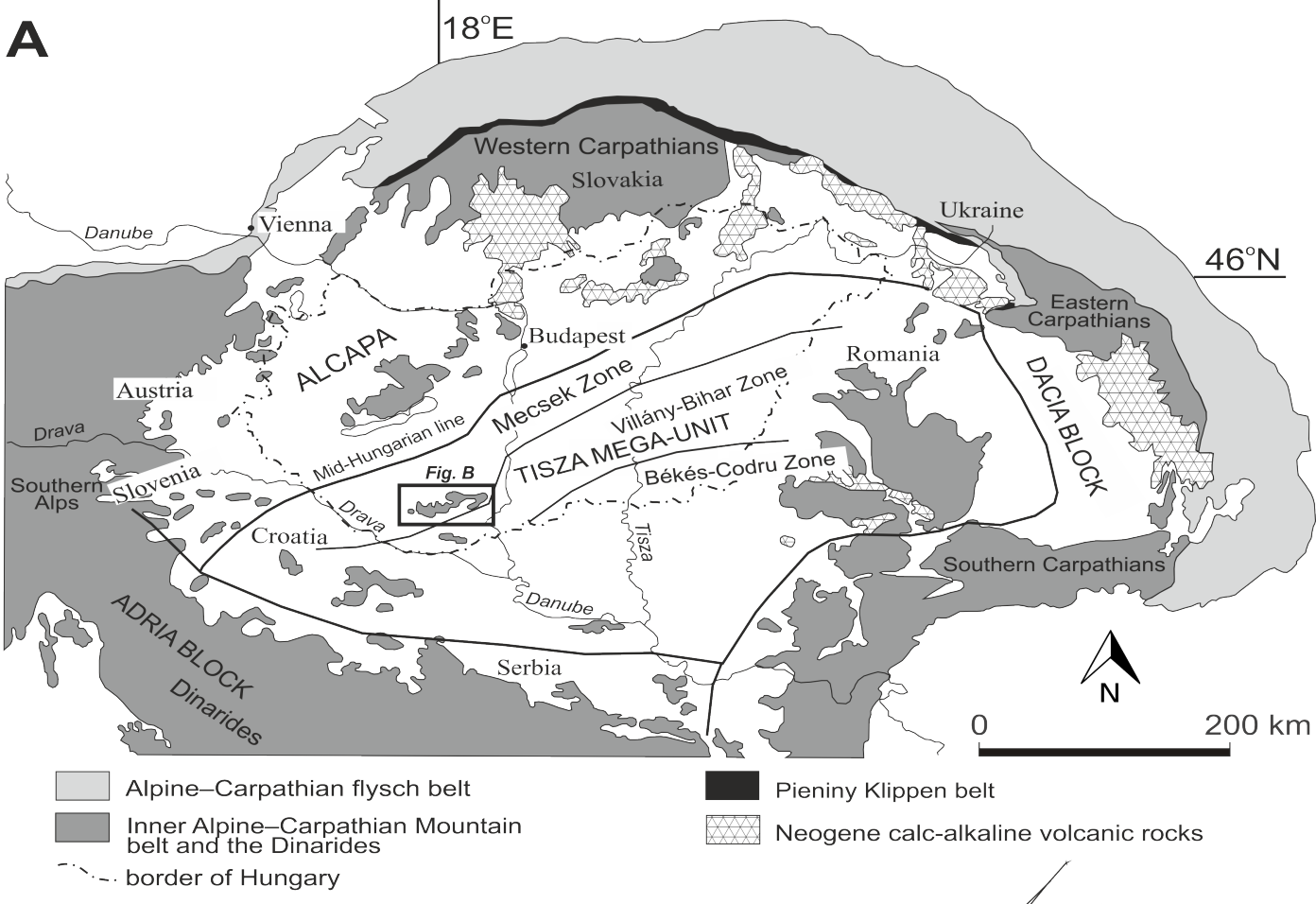
A
18°E
Western Carpathians
Slovakia
Ukraine
Danube
Vienna
46°N
Eastern Carpathians
Budapest
ALCAPA
Romania
Austria
Mecsek Zone
Villány-Bihar Zone
DACIA BLOCK
Drava
Mid-Hungarian line
TISZA MEGA-UNIT
Fig. B
Southern Alps
Slovenia
Békés-Codru Zone
Drava
Croatia
Tisza
Southern Carpathians
Danube
ADRIA BLOCK
Dinarides
Serbia
N
0
200 km
Alpine–Carpathian flysch belt
Pieniny Klippen belt
Inner Alpine–Carpathian Mountain belt and the Dinarides
Neogene calc-alkaline volcanic rocks
border of Hungary

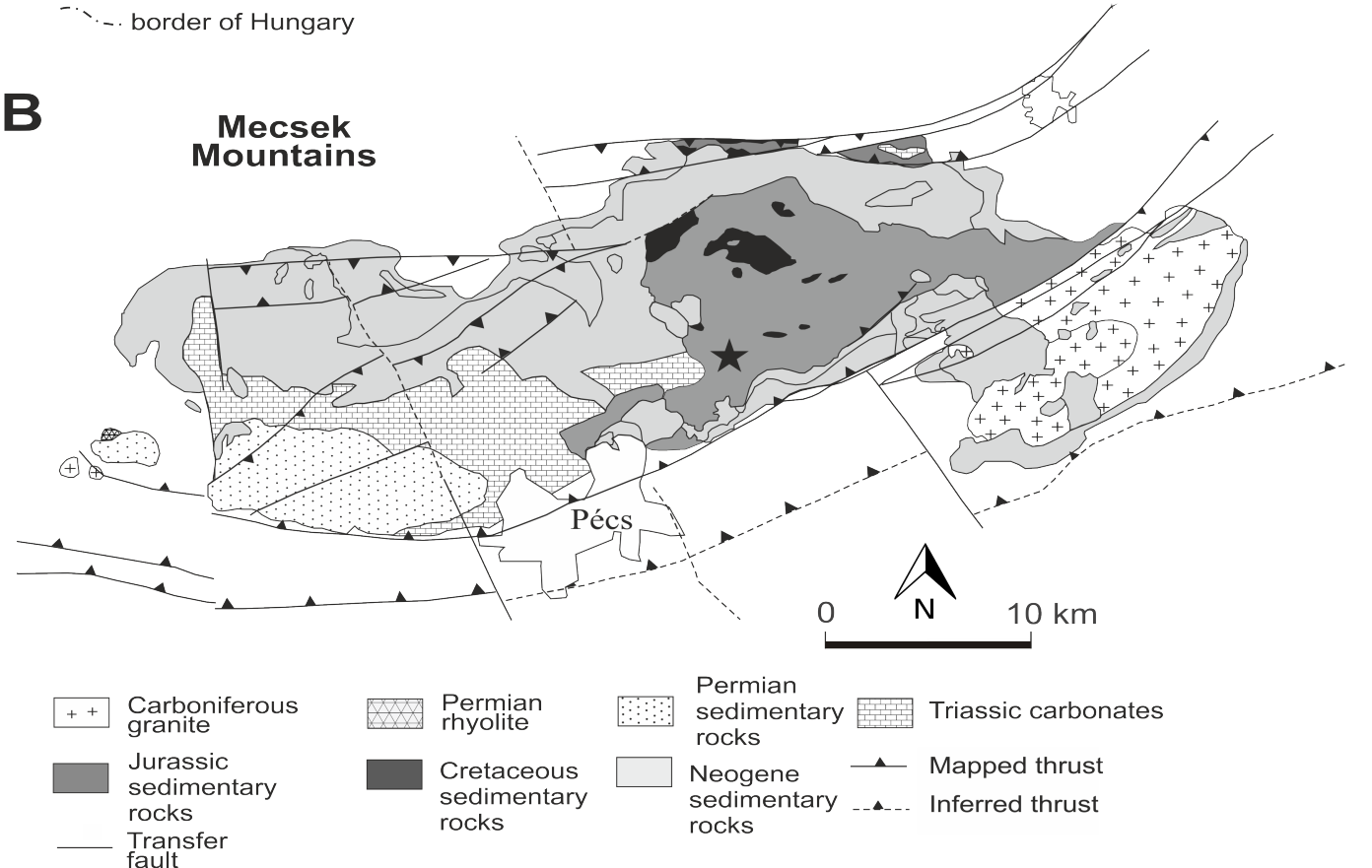
B
Mecsek Mountains
Pécs
N
0
10 km
Carboniferous granite
Permian rhyolite
Permian sedimentary rocks
Triassic carbonates
Jurassic sedimentary rocks
Cretaceous sedimentary rocks
Neogene sedimentary rocks
Mapped thrust
Inferred thrust
Transfer fault

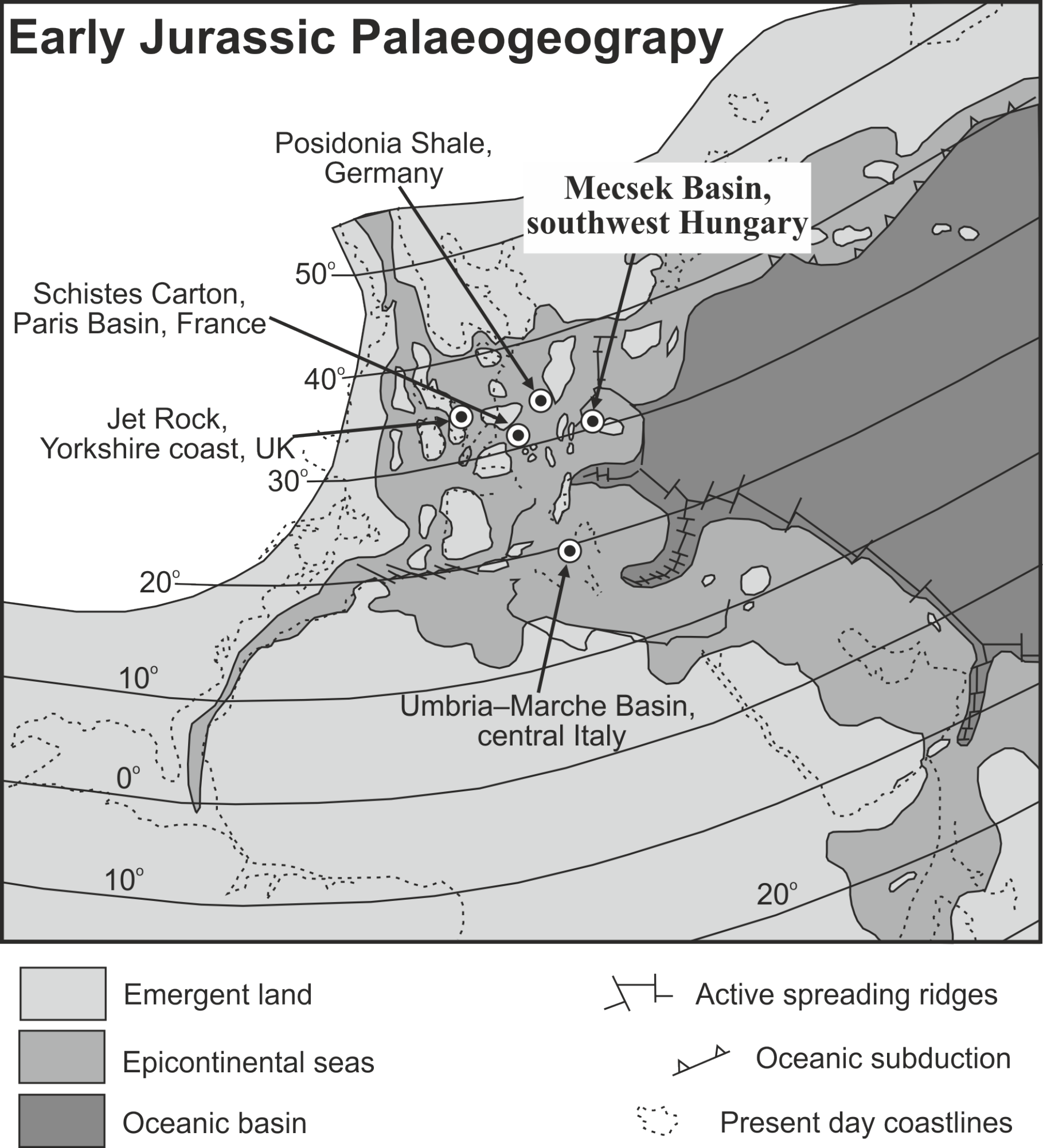
Early Jurassic Palaeogeograpy
Posidonia Shale, Germany
Mecsek Basin, southwest Hungary
50°
Schistes Carton, Paris Basin, France
40°
Jet Rock, Yorkshire coast, UK
30°
20°
10°
Umbria–Marche Basin, central Italy
0°
10°
20°
Emergent land
Epicontinental seas
Oceanic basin
Active spreading ridges
Oceanic subduction
Present day coastlines

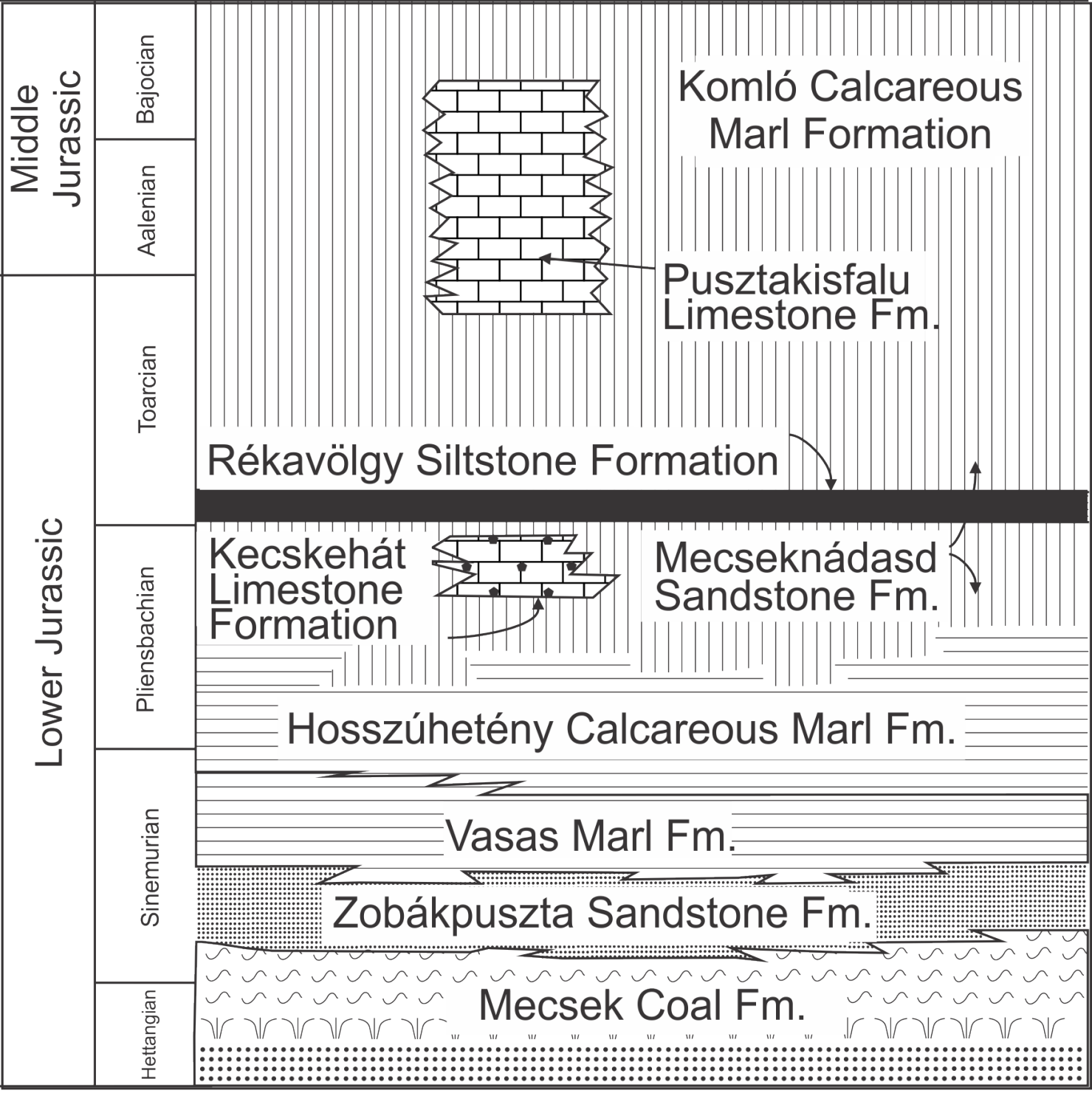

fluvial

swamp

lagoon

open shelf

debris flow

shallow marine carbonates

black shale

hemipelagic sediments

shallow marine siliciclastic sediments

Fm. Formation

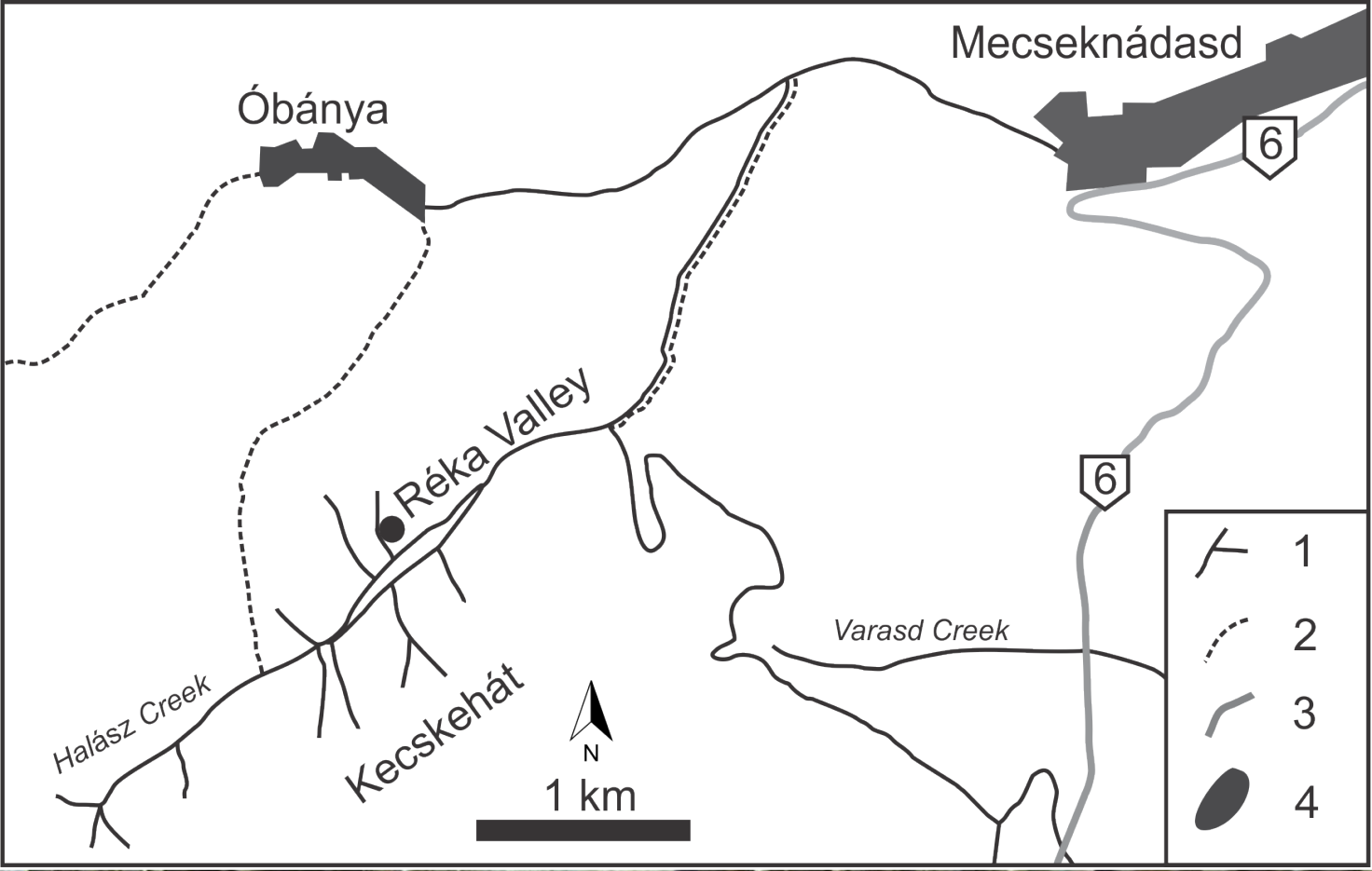
Mecseknádasd
Óbánya
6
Réka Valley
6
1
2
3
4
Varasd Creek
Halász Creek
Kecskehát
N
1 km

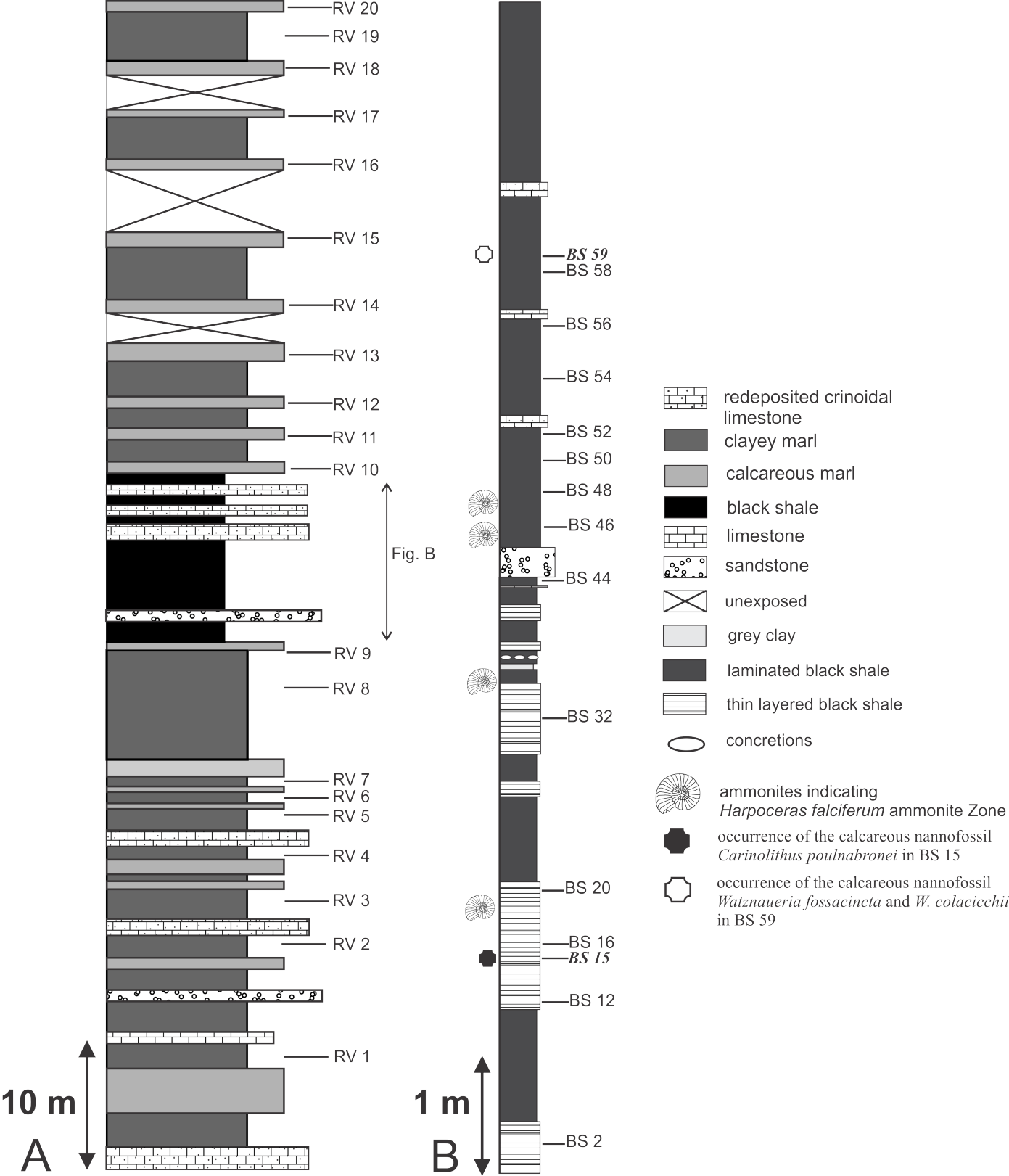
RV 20
RV 19
RV 18
RV 17
RV 16
RV 15
RV 14
RV 13
RV 12
RV 11
RV 10
Fig. B
RV 9
RV 8
RV 7
RV 6
RV 5
RV 4
RV 3
RV 2
RV 1
10 m
A
BS 59
BS 58
BS 56
BS 54
BS 52
BS 50
BS 48
BS 46
BS 44
BS 32
BS 20
BS 16
BS 15
BS 12
BS 2
1 m
B
redeposited crinoidal limestone
clayey marl
calcareous marl
black shale
limestone
sandstone
unexposed
grey clay
laminated black shale
thin layered black shale
concretions
ammonites indicating Harpoceras falciferum ammonite Zone
occurrence of the calcareous nannofossil Carinolithus poulnabronei in BS 15
occurrence of the calcareous nannofossil Watznaueria fossacincta and W. colacicchii in BS 59

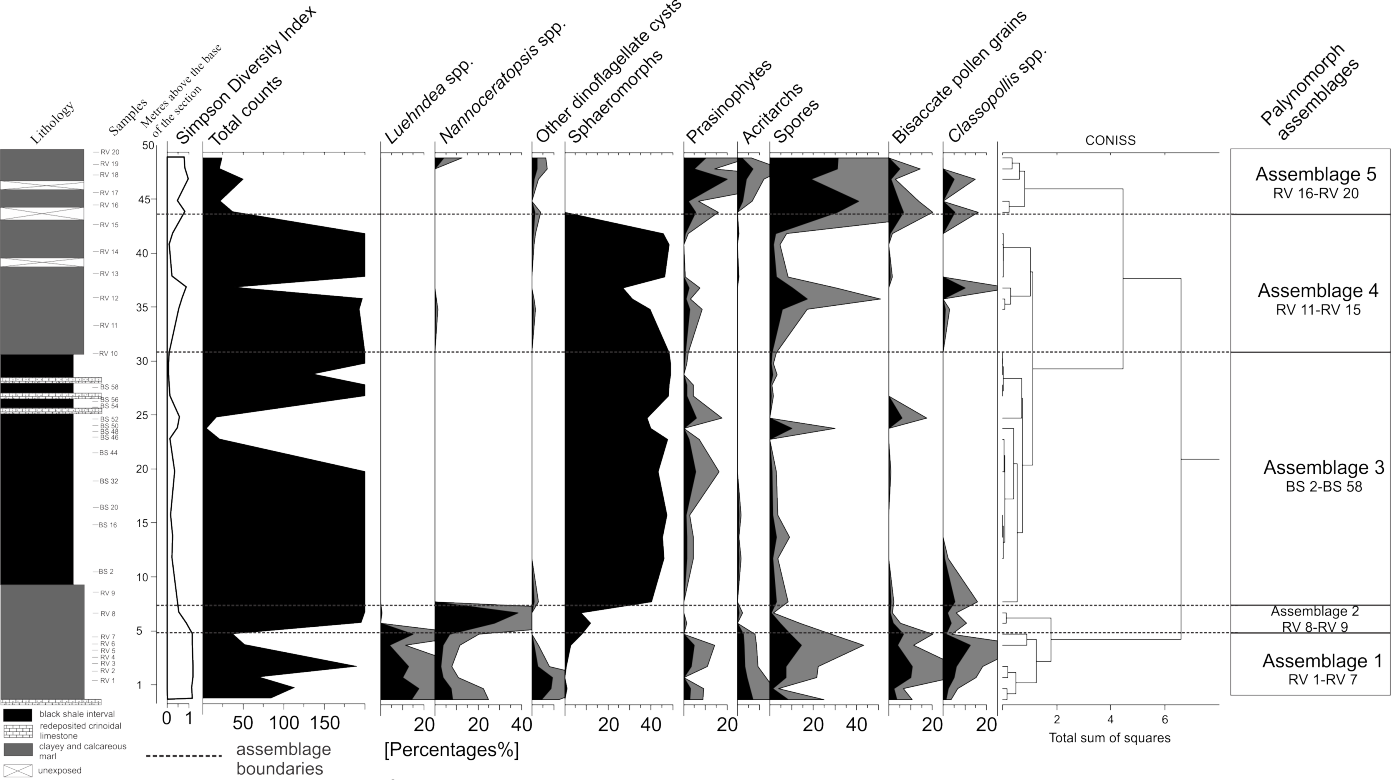
Lithology
Samples
Metres above the base of the section
Simpson Diversity Index
Total counts
Luehndea spp.
Nannoceratopsis spp.
Other dinoflagellate cysts
Sphaeromorphs
Prasinophytes
Acritarchs
Spores
Bisaccate pollen grains
Classopollis spp.
CONISS
Palynomorph assemblages
Assemblage 5
RV 16-RV 20
Assemblage 4
RV 11-RV 15
Assemblage 3
BS 2-BS 58
Assemblage 2
RV 8-RV 9
Assemblage 1
RV 1-RV 7
black shale interval
redeposited crinoidal limestone
clayey and calcareous marl
unexposed
assemblage boundaries
[Percentages%]
Total sum of squares

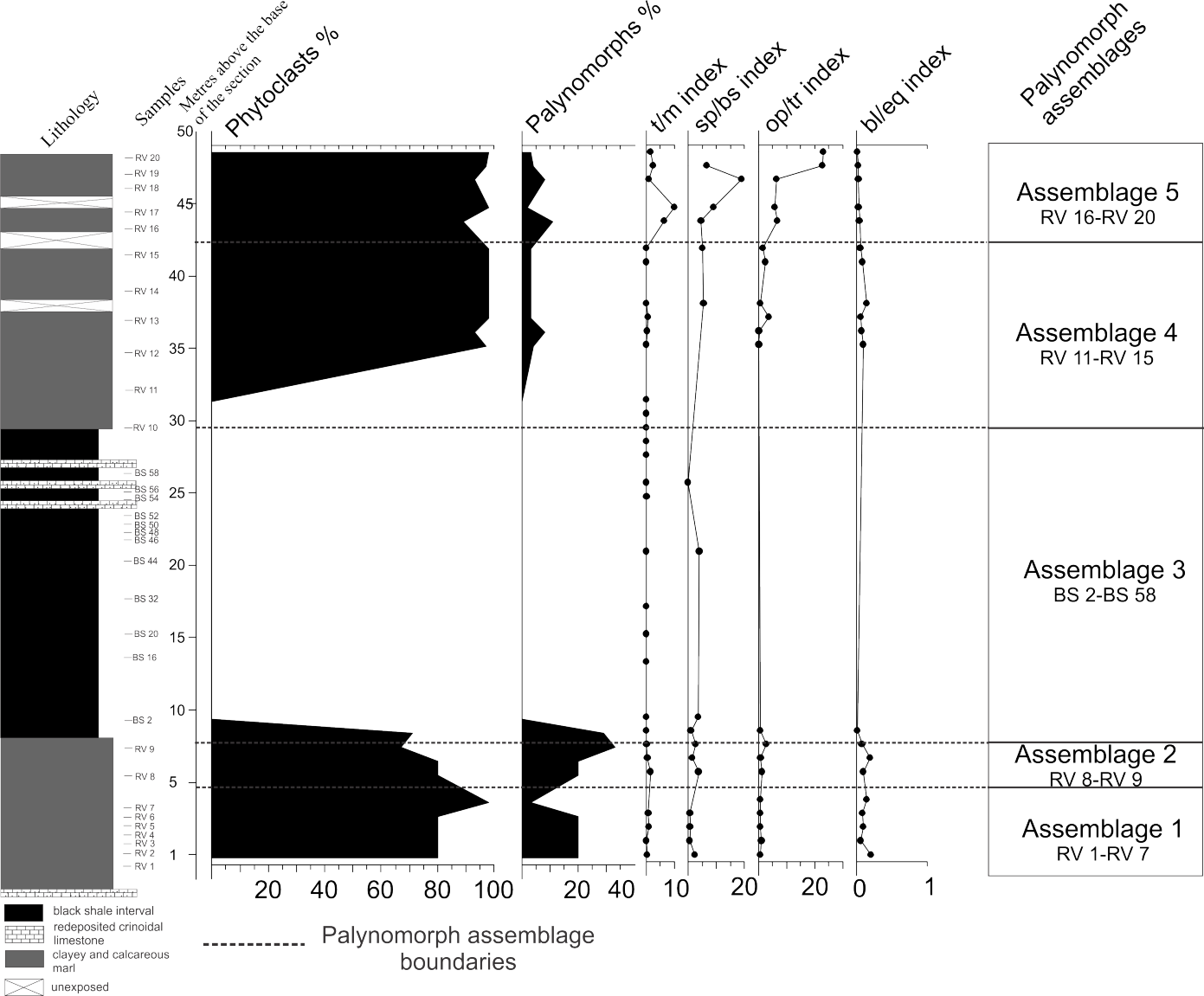
Lithology
Samples
Metres above the base of the section
Phytoclasts %
Palynomorphs %
t/m index
sp/bs index
op/tr index
bl/eq index
Palynomorph assemblages
RV 20
RV 19
RV 18
RV 17
RV 16
RV 15
RV 14
RV 13
RV 12
RV 11
RV 10
BS 58
BS 56
BS 54
BS 52
BS 50
BS 48
BS 46
BS 44
BS 32
BS 20
BS 16
BS 2
RV 9
RV 8
RV 7
RV 6
RV 5
RV 4
RV 3
RV 2
RV 1
50
45
40
35
30
25
20
15
10
5
1
20 40 60 80 100
20 40
10 20
20
0 1
Assemblage 5
RV 16-RV 20
Assemblage 4
RV 11-RV 15
Assemblage 3
BS 2-BS 58
Assemblage 2
RV 8-RV 9
Assemblage 1
RV 1-RV 7
black shale interval
redeposited crinoidal limestone
clayey and calcareous marl
unexposed
Palynomorph assemblage boundaries

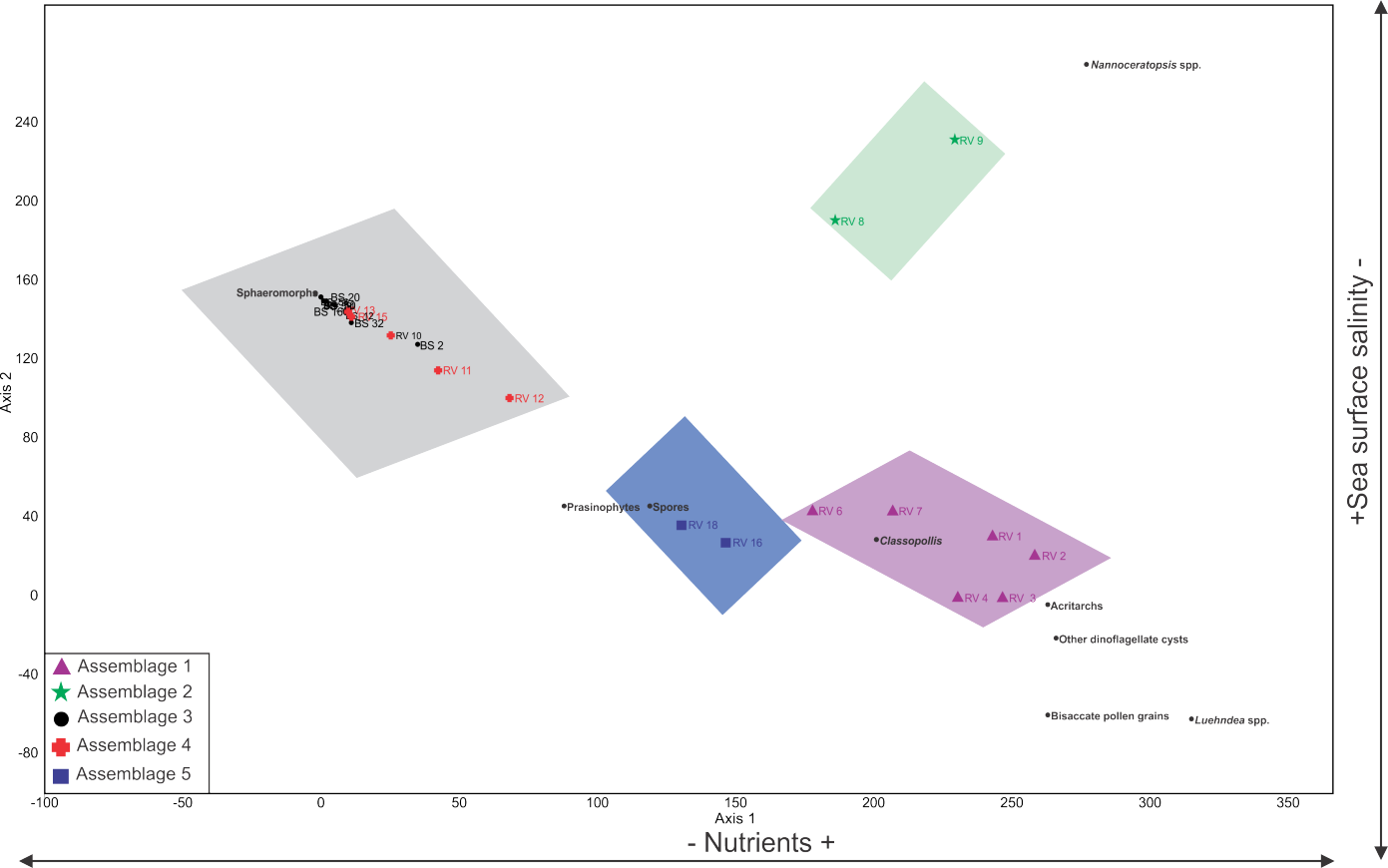
Nannoceratopsis spp.
RV 9
RV 8
Sphaeromorphe
BS 20
BS 32
RV 10
BS 2
RV 11
RV 12
Prasinophytes
Spores
RV 18
RV 16
RV 6
RV 7
Classopollis
RV 1
RV 2
RV 4
RV 3
Acritarchs
Other dinoflagellate cysts
Bisaccate pollen grains
Luehndea spp.
Assemblage 1
Assemblage 2
Assemblage 3
Assemblage 4
Assemblage 5
Axis 2
240
200
160
120
80
40
0
-40
-80
-100
-50
0
50
100
150
200
250
300
350
Axis 1
- Nutrients +
+Sea surface salinity -

Palynofacies terminology	
Sedimentary organic particles	**Description**
Amorphous organic matter (AOM)	Structureless, irregularly shaped, fluffy yellowish-brown to black masses that can be derived from the degradation of terrestrial or marine organic matter.
Charcoal/black debris	Totally opaque particles with variable shape and size. They are derived from highly oxidised wood or other plant debris.
Structured translucent plant debris	Structured transparent particles with yellow-green to brown colour. They may be derived from degraded plant tissues or wood. They are of various shape and size including lath-shaped and equidimensional particles. As cuticles are extremely scarce in the investigated material, they were counted as part of this group.
Spores	Male reproductive organs of bryophytes and pteridophytes
Pollen grains	Male reproductive organs of the seed plants
Marine palynomorphs	Dinoflagellate cysts, acritarchs, prasinophytes, spheromorphs and chitinous inner linings of foraminifera
Palynofacies indices	
t/m index	The t/m index quantifies the ratio of terrestrial (t) to marine (m) palynomorphs, which reflects the vegetation of the hinterland and the proportion of terrigenous input
sp/bs index	The bs/sp index measures the ratio of spores (sp) to bisaccate pollen grains (bs).
op/tr index	The op/tr index quantifies the ratio of opaque (op) to translucent (tr) phytoclasts. It can indicate changes in the depositional environment, as it reflects shifts between proximal and distal settings.
bl/eq index	The bl/eq index measures the ratio of bladed-lath shaped (bl) and equidimensional (eq) opaque phytoclasts, which also captures proximal/distal trends.

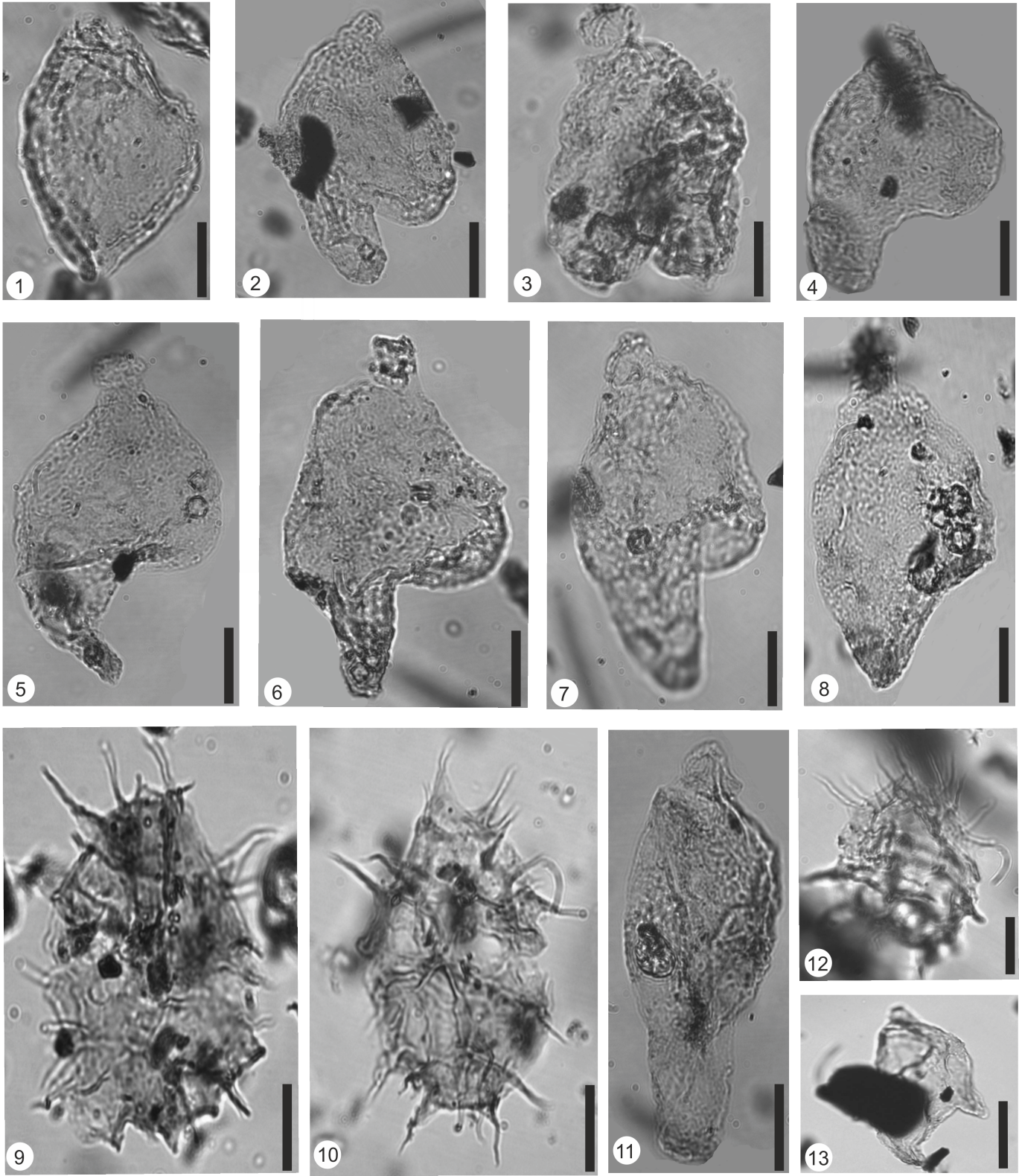
1
2
3
4
5
6
7
8
9
10
11
12
13

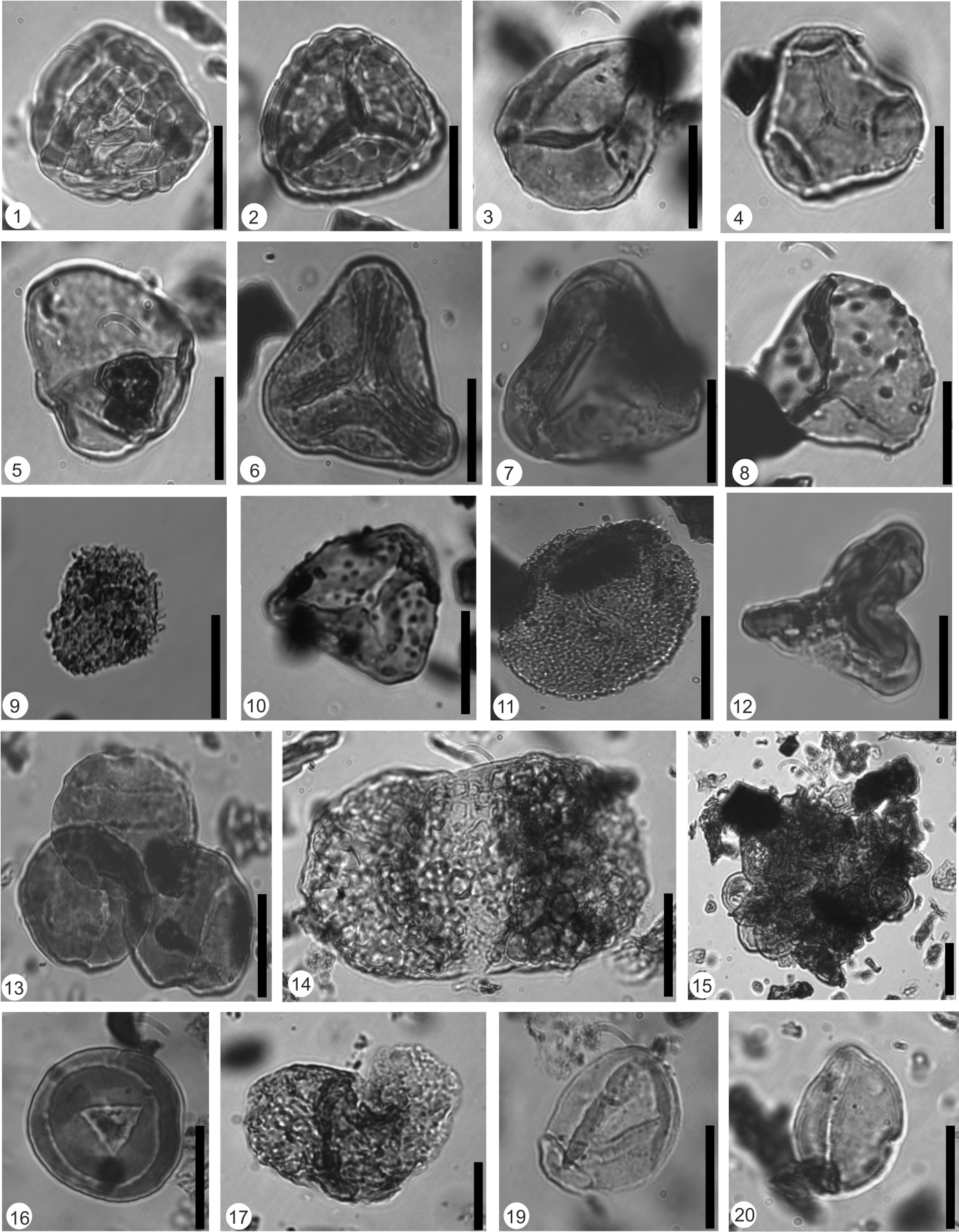
1
2
3
4
5
6
7
8
9
10
11
12
13
14
15
16
17
19
20

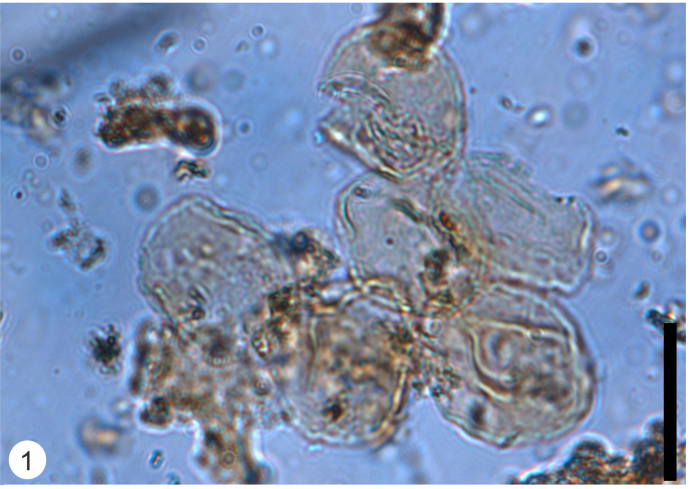
1

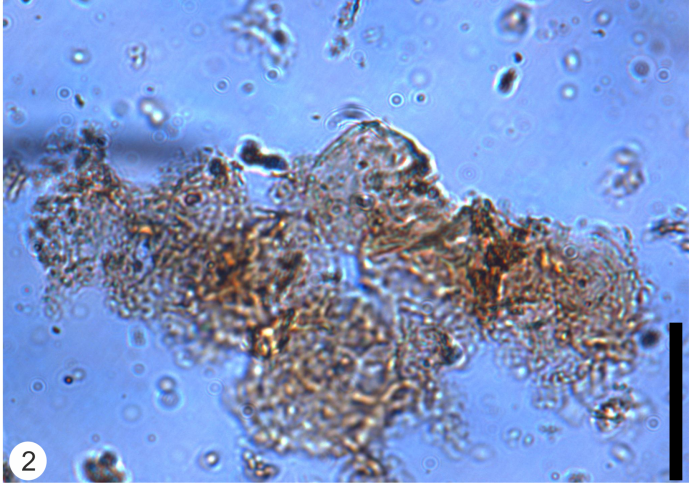
2

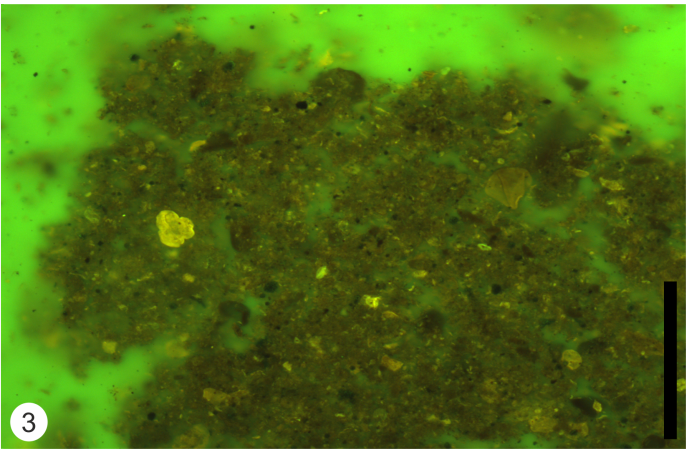
3

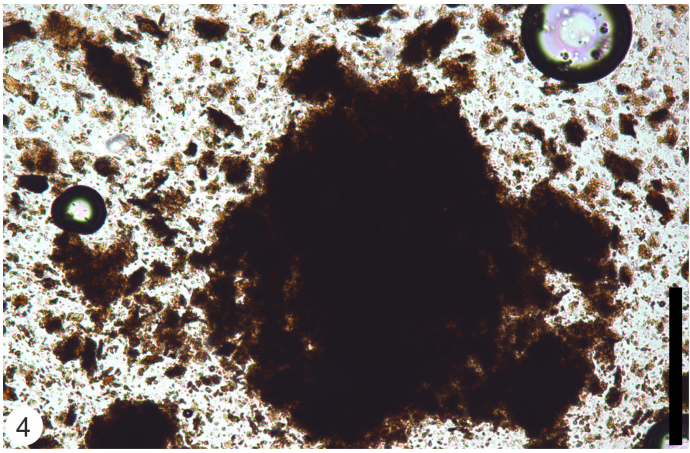
4

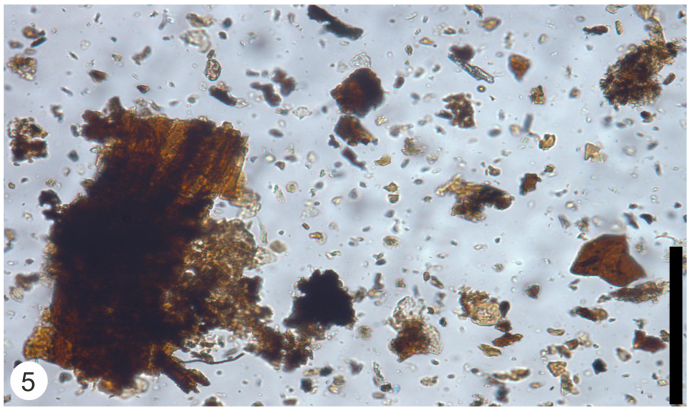
5

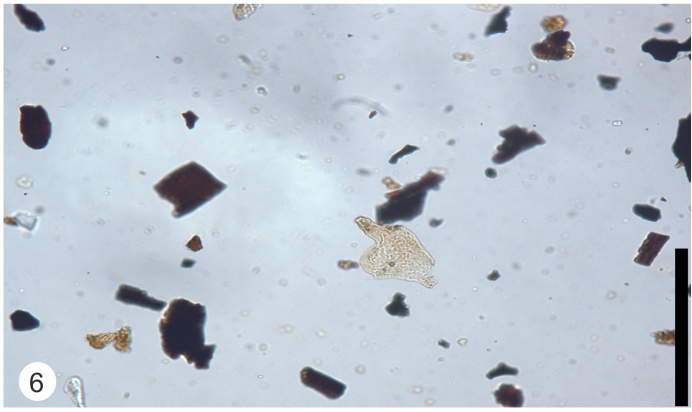
6

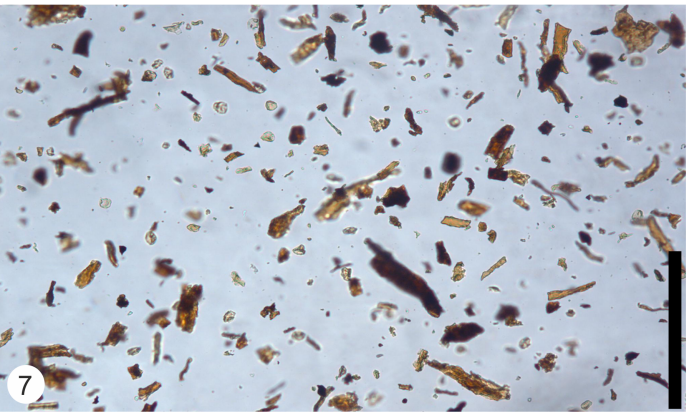
7

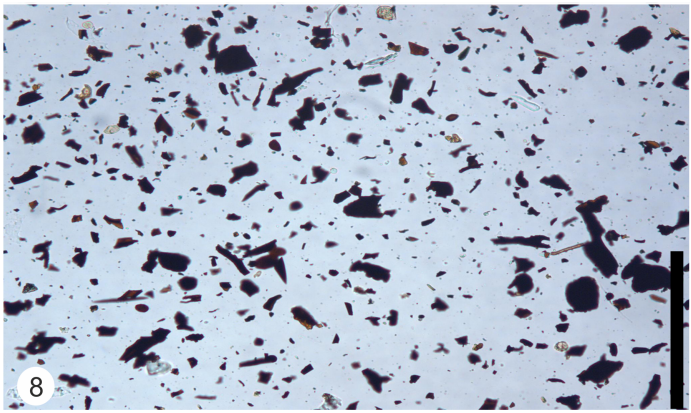
8

File(s) excluded from PDF

The following file(s) will not be converted:

table 2.tif

Please click 'Download zip file' to download the most recent files related to this submission.